

Oligoaniline-Functionalized terpyridine ligands and their ruthenium(II) complexes: synthesis, spectroscopic property and redox behavior†

Dongfang Qiu,^{a,b} Yanxiang Cheng^{*a} and Lixiang Wang^{*a}

Received 14th November 2008, Accepted 18th February 2009

First published as an Advance Article on the web 13th March 2009

DOI: 10.1039/b820392j

A series of oligoaniline-functionalized mono- and bis-topic terpyridine ligands, *i.e.* C₆H₅[N(R)C₆H₄]_nTPY (R = H, butyl, *tert*-butyloxycarbonyl; *n* = 1–4; TPY = 2,2':6',2''-terpyridyl) and TPYC₆H₄[N(R)C₆H₄]_mTPY (R = H, *tert*-butyloxycarbonyl; *m* = 2, 4), and the corresponding mono- and bis-nuclear ruthenium(II) complexes have been synthesized and verified. The spectroscopic results indicate that two kinds of π – π^* transitions from TPY and oligoaniline fragments of ligands strongly shift to lower energy, and the metal-to-ligand charge-transfer transition (¹MLCT) bands of all obtained complexes are considerably red-shifted ($\Delta\lambda_{\text{max}} = 22$ –64 nm) and their intensities become much more intense (approximately 4–6 times), compared with those of the reported complex [Ru(TPY)₂]²⁺. Moreover, the spectroscopic properties of the ligands and complexes with longer oligoaniline units (*n* = 3, 4) are markedly influenced by the external stimulus, such as the oxidation and proton acid doping. The characteristic absorption bands in the visual and near infrared (NIR) scales demonstrate the presence of various oxidized and doped states of the oligoaniline unit. All complexes show multiplicate redox processes based on metal center, oligoaniline and terpyridine units. The potential shifts suggest the donor and acceptor (D–A) interaction between the oligoaniline unit and the bis(terpyridine)–Ru²⁺ center.

Introduction

2,2':6',2''-Terpyridine (TPY) transition metal complexes have attracted much attention because of their wide applications in modern coordination chemistry, biology and material science.^{1,2} Motivated by the fact that the photophysical and redox properties of TPY–metal complexes depend on the substituent in the ligand, a great advance has been made in the design of terpyridine derivatives.³ Introducing the functional groups at the 4'-position of terpyridine is the main pathway, due to the synthetic convenience and the geometrical advantage. In recent years, a novel class of bis-topic terpyridine ligands (T-S-T), where two terpyridine units (T) are linked in the back-to-back configuration (*via* their 4' positions) by a rigid spacer (S), shows a huge potential in the supermolecular chemistry.⁴ Various saturated⁵ or conjugated components, such as azobenzene,⁶ diarylethenes,⁷ polyacetylenes,⁸ poly(phenylene-ethynyls),⁹ thiophenes,¹⁰ oligo(diethynyl-thiophenes),¹¹ and oligoferrocenes,¹² have been utilized as spacers to incorporate into d⁶ transition metal [Ru(II), Os(II), Rh(III) and Ir(III)] terpyridyl complexes. The rod-like homonuclear and heteronuclear complexes are suitable to simply mimic the photoinduced electron and energy transfer process in the natural system.¹³ Concerning the electronic characteristics, the saturated spacers are responsible

for a remarkable attenuation of the intercenter interaction, while the unsaturated and conjugated spacers appear to have good conducting properties. The spectroscopic and electrochemical properties of the homonuclear complexes are obviously improved due to the interaction between the spacer and metal–TPY unit. The vectorial electron- or energy-transfer rate between the donor and acceptor in the heteronuclear complex can be modulated by tuning the length and the nature of the spacer.

Oligoaniline is usually used as a modular system to understand clearly the electrical and optical properties of polyaniline because of its monodisperse composition and well-defined structure. Like polyaniline,¹⁴ oligoaniline also has various forms, such as the leucoemeraldine base (LEB), emeraldine base (EB), emeraldine salt (ES) and pernigraniline base (PNB), which can be easily controlled by simple redox and acid–base reactions,¹⁵ as shown in Fig. 1. The difference of electronic and/or chemical structures among the various forms gives rise to remarkable changes in electrical and optical properties, which suggests that oligoaniline is a promising class as a photo- and electro-active unit for the functionalization of the terpyridine systems. In this paper, we synthesized a novel series of mono- and bis-topic terpyridine ligands with oligoanilines as functional group and spacer, respectively, and the corresponding mono- and bis-nuclear ruthenium(II) complexes. The basic studies on their spectroscopic and electrochemical behaviors are: (i) to investigate the donor–acceptor (D–A) interaction between the oligoaniline and TPY or metal–TPY moieties by changing the chain length (*n*) and the substituted group in the oligoaniline unit, (ii) to learn about the influence of the changed electronic and chemical structure in the oligoaniline unit, resulting from various external stimuli. The information obtained about the relationship between the chemical/electronic structures of oligoanilines and photo/electro-properties of complexes should

^aState Key Laboratory of Polymer Physics and Chemistry, Changchun Institute of Applied Chemistry, Chinese Academy of Sciences, Changchun, 130022, P. R. China. E-mail: yanxiang@ciac.jl.cn, lixiang@ciac.jl.cn; Fax: +86-431-85684937; Tel: +86-431-85262106

^bGraduate University of the Chinese Academy of Sciences, Chinese Academy of Sciences, Beijing, 100039, P. R. China

† Electronic supplementary information (ESI) available: Experimental details. CCDC reference number 691744. For ESI and crystallographic data in CIF or other electronic format see DOI: 10.1039/b820392j

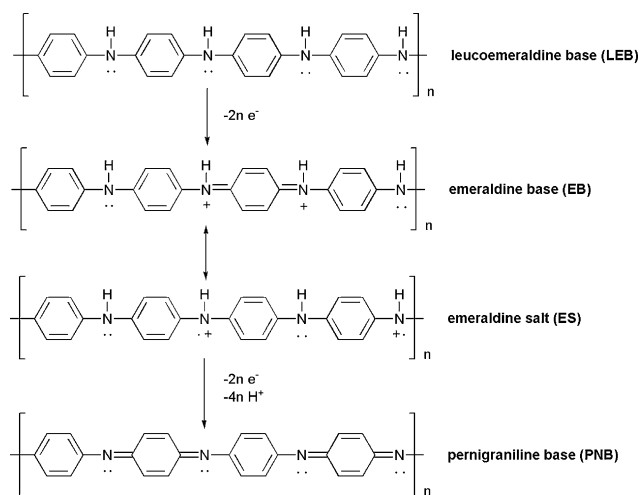


Fig. 1 Principal oxidation states of polyaniline and oligoaniline.

provide a solid basis for further research into the heteronuclear system.

Results and discussion

Ligand synthesis

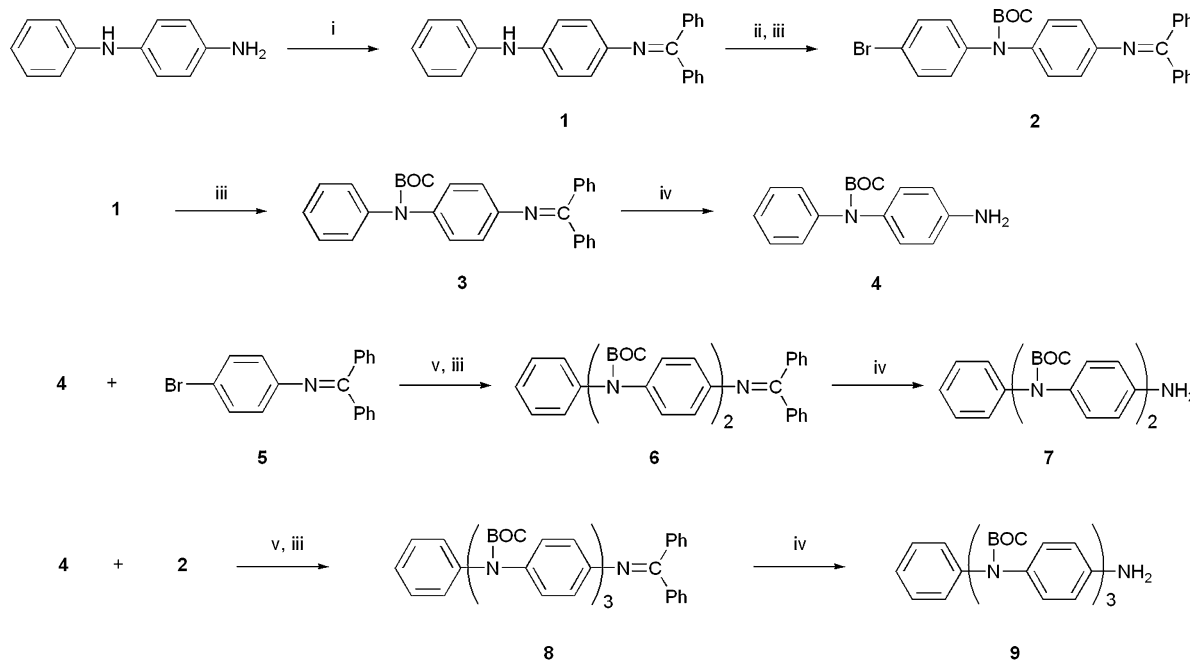
In order to facilitate the condensation with the 4'-(4-bromophenyl)-2,2': 6',2''-terpyridine, the synthesis of aniline oligomers with an $-NH_2$ functional end group is a key factor. Compared with other methods,¹⁶ the palladium-catalyzed amination,¹⁷ which was reported as an efficient pathway to synthesize the aniline oligomers with different functional end groups, can meet the need. Several catalyst systems have been used in this method.^{17,18}

Among them, the $Pd(OAc)_2/DPEphos$ ($DPEphos = bis[(2-diphenylphosphino)phenyl]ether$) system has some advantages over other catalyst/ligand systems, such as the catalyst and ligand are stable in air and not very expensive. Therefore, we adopted the $Pd(OAc)_2/DPEphos$ system to synthesize the oligoanilines and oligoaniline-functionalized terpyridines. Compounds **1**, **2**, **3**, **6**, **8**¹⁹ (Scheme 1) and **12**^{17c} (Scheme 3) were prepared according to literature methods with improved experimental conditions. Compounds **4**, **7**, **9** and **13** were recovered by palladium-catalyzed hydrogenation from the precursors **3**, **6**, **8** and **12** in excellent yield (>90%), respectively.

The syntheses of the ligands explored in this work are shown in Schemes 2 and 3. Aniline or 1,4-phenylenediamine directly coupled with 1 or 2 eq. of compound **10**,²⁰ followed by protection with BOC groups, affording **L**⁷ in 84% yield or **L**¹¹ in 62% yield. Compounds **4**, **7**, **9** and **13** were coupled with compound **10** via the same way to afford the BOC-substituted ligands **L**⁸, **L**⁹, **L**¹⁰ and **L**¹² in good yields (69–88%). These results suggest that the catalyst system $Pd(OAc)_2/DPEphos$ is also highly efficient for the synthesis of oligoaniline-functionalized terpyridines. The reduced state ligands **L**^{1–6}, in which the oligoaniline units are in the LEB form, were generally prepared by thermolysis of the BOC-substituted ligands under an inert atmosphere at 185 °C for 12 h²¹ or by treatment of the precursors with TMSI²² at room temperature in DCM solution. **L**¹ and **L**² reacted with excess 1-bromobutane to afford the Bu-substituted ligands **L**¹³ and **L**¹⁴ in very good yields (>90%), respectively.

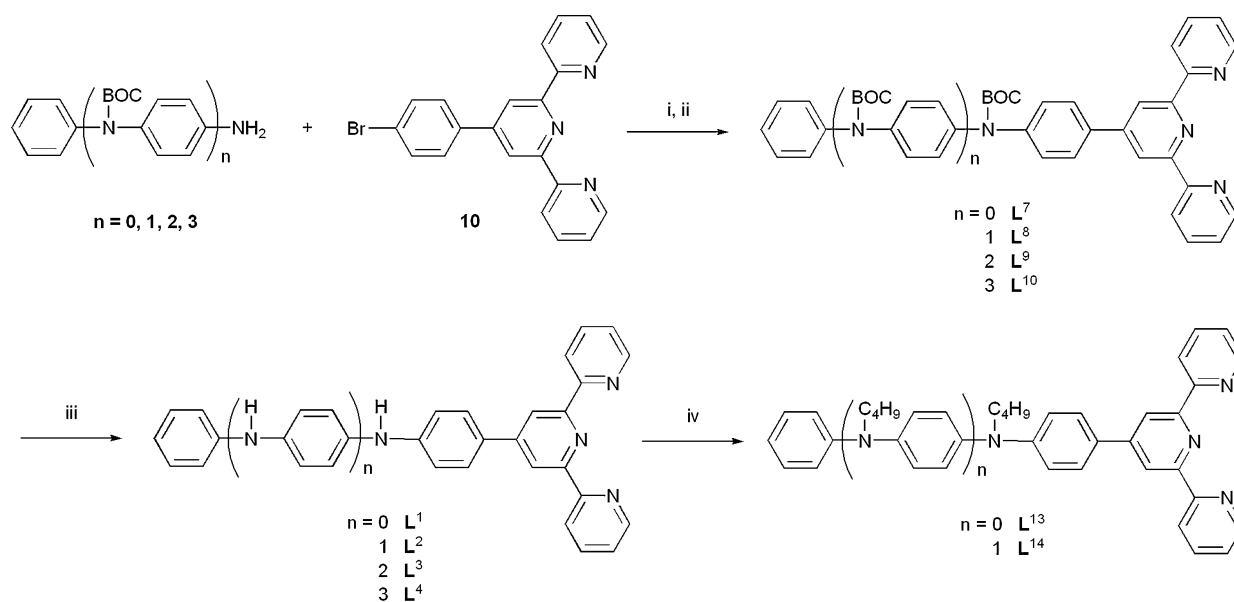
Complex synthesis

Fig. 2 shows the general structure of the modular systems. The BOC- and Bu-substituted mononuclear Ru(II) complexes were prepared by the direct reaction of metal chloride with 2 eq.



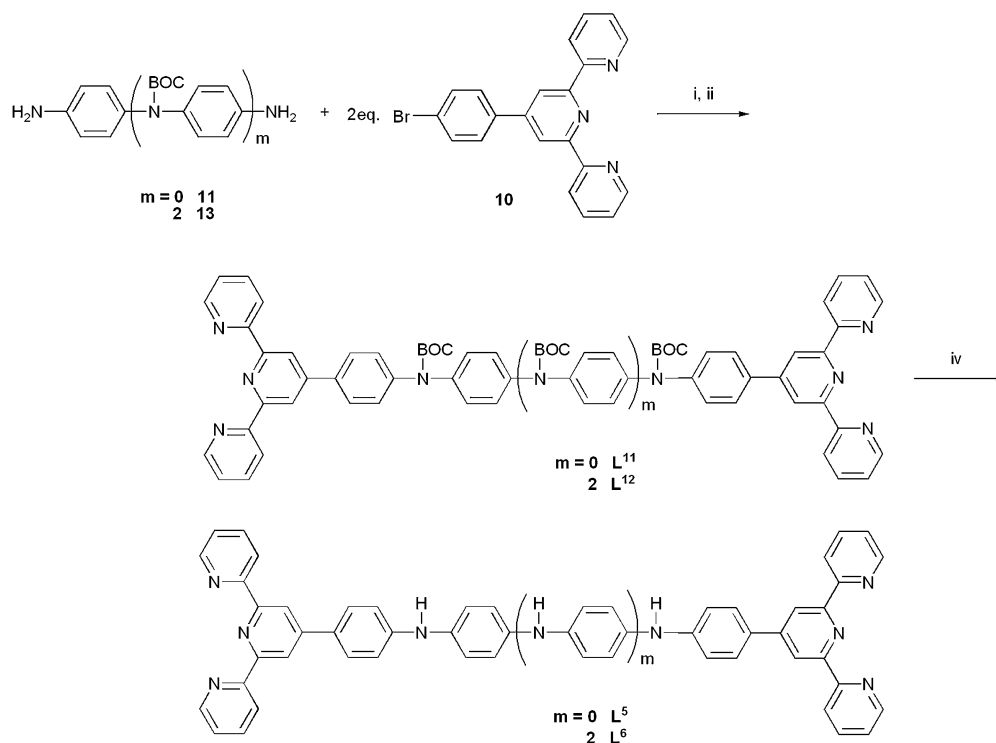
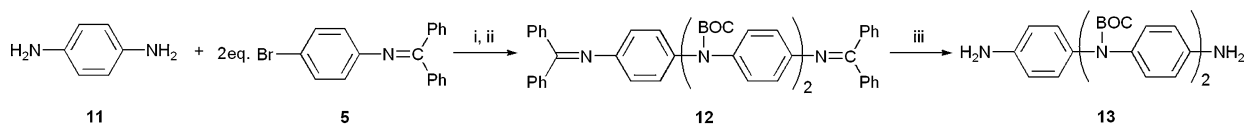
(i) Ph_2CO , toluene, reflux, 48 h; (ii) $n-Bu_4NBr_3$, CH_2Cl_2 , rt, 1 h; (iii) $(BOC)_2O$, DMAP, THF, reflux, 24 h; (iv) NH_4HCO_2 , Pd/C , THF/MeOH, reflux, 30 min; (v) $Pd(OAc)_2$, $DPEphos$, $NaOBu^t$, THF, reflux, 24 h.

Scheme 1



(i) (BOC)₂O, DMAP, THF, reflux, 24 h; (ii) Pd(OAc)₂, DPEphos, NaOBu^t, THF, reflux, 24 h; (iii) 185 °C, Ar, 12 h; (iv) NaH, C₄H₉Br, THF, 50 °C, 24 h.

Scheme 2



(i) Pd(OAc)₂, DPEphos, NaOBu^t, THF, reflux, 24 h; (ii) (BOC)₂O, DMAP, THF, reflux, 24 h; (iii) NH₄HCO₂, Pd/C, THF/MeOH, reflux, 30 min; (iv) 185 °C, Ar, 12 h.

Scheme 3

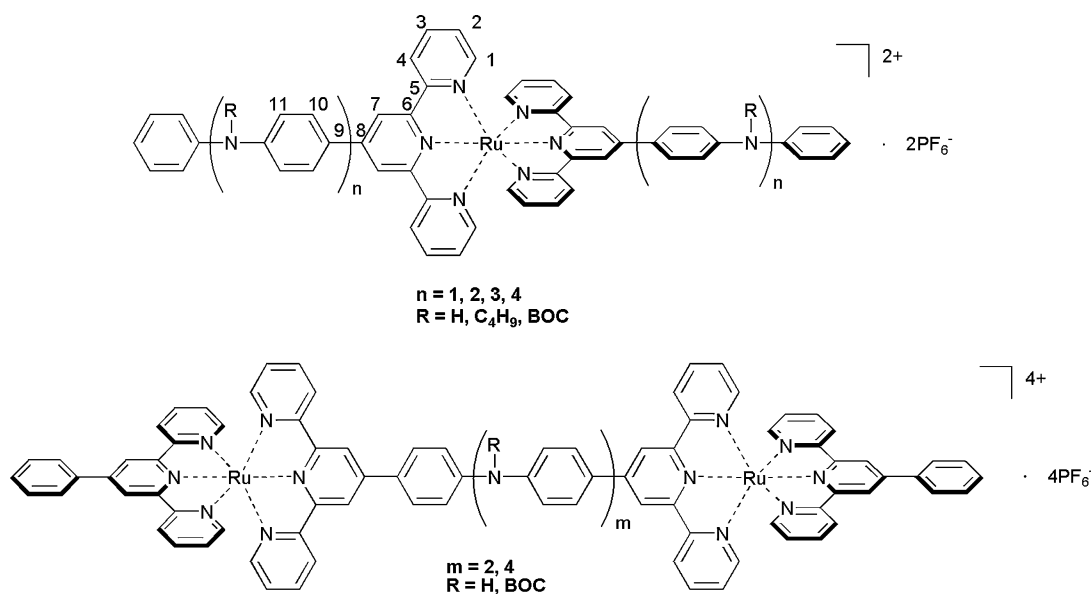


Fig. 2 Molecular structures of the mono- and dinuclear Ru(II) complexes.

mono-topic ligands L^7 – L^{10} , L^{13} and L^{14} , respectively, in EtOH solutions containing a small amount of *N*-ethylmorpholine as a reducing agent, followed by precipitation of the hexafluorophosphate salts and chromatographic purification. Treatment of bis-topic ligands L^{11} and L^{12} with two times the amount of $[Ru(PTPY)Cl_3]$ (PTPY = 4'-phenyl-2,2':6',2''-terpyridyl) via the same way resulted in the formation of the symmetric dinuclear complexes. All of the complexes exhibit well-resolved 1H NMR spectra, in which a number of characteristic peaks are present and agree with those of other reported Ru(II) complexes with 4'-substituted terpyridyl ligands.²³ In the heteroleptic dinuclear complexes $\{[(PTPY)Ru(L^5)Ru(PTPY)](PF_6)_4$ and $[(PTPY)Ru(L^6)Ru(PTPY)](PF_6)_4\}$, split *dd* peaks are observed for both terpyridyl domains (see Fig. S1 and S2 in the ESI†).

The reduced state mono- or dinuclear Ru(II) complexes, in which the oligoaniline units are in the LEB form, were obtained by thermolysis of the BOC-substituted complexes under an inert atmosphere at 185 °C for 12 h or by treatment of the precursors with TMSI at room temperature in MeCN solution except for $[(PTPY)Ru(L^6)Ru(PTPY)](PF_6)_4$, which was decomposed during the deprotection process. The yields are quantitative and the structures of these complexes were easily confirmed by the proton signals at 7–9 ppm from NH groups (see Fig. S3 in the ESI†).

Crystal structure of $[Ru(L^{13})_2](PF_6)_2$

By using the slow evaporation method, red crystals of $[Ru(L^{13})_2](PF_6)_2$ were deposited from its concentrated solution in the acetone–methanol system. The molecular structure of the cation and numbering scheme adopted are depicted in Fig. 3. Selected bond length and angle data are presented in Table 1.

The ruthenium(II) ion displays the expected distorted-octahedral geometry with intraligand bite angles (N–Ru–N) in the range 78.5(3)–79.3(3)°. The two terpyridyl units are approximately planar with 0.1–5.6° torsional angles (N–C–N) between terminal and central pyridyl rings. The angle between the least-square planes of central pyridyl rings from the two terpyridyl

ligands is 88.8° and the angle formed by the Ru atom and the nitrogen atoms of the central pyridyl groups (N2–Ru–N5) is 176.8(4)°. The torsional angles between the central pyridyl ring of the terpyridyl and the linked phenyl ring are 18.1° (C9–C8–C16–C21) and 27.5° (C40–C39–C47–C48), respectively. The sp^3 hybridized nitrogen atom and directly bonded three carbon atoms from the two phenyl and butyl groups nearly form a plane with the torsional angles 177.7° (C19–C22–C28–N7) and 168.6° (C50–C53–C59–N8). All C–N and C–C distances of the $[Ru(TPY)_2]$ moiety are in the normal range. The Ru–N distances are similar to those reported in the literature,² and the bonds to the central pyridyl rings [1.982(7), 1.986(7) Å] are evidently shorter than those to the terminal pyridyl rings [2.049(6)–2.069(8) Å]. The cations lie on two different columns which partly overlap each other and there are two forms of π – π stacking interactions between adjacent cations in the crystal packing (Fig. 3). The face-to-face contacts (C4–C13', 3.32; C3–C14', 3.51 Å) between the two terminal pyridyl rings of neighbouring terpyridyl groups are present in an identical column, while the edge-to-face contacts (C13–C52'', 3.58;

Table 1 Selected bond distances (Å) and bond angles (°) for $[Ru(L^{13})_2](PF_6)_2$

Ru–N1	2.057(7)	N2–Ru–N3	78.8(3)
Ru–N2	1.982(7)	N2–Ru–N4	102.2(3)
Ru–N3	2.062(6)	N2–Ru–N5	176.8(4)
Ru–N4	2.049(6)	N2–Ru–N6	99.9(3)
Ru–N5	1.986(7)	N3–Ru–N4	87.9(2)
Ru–N6	2.069(8)	N3–Ru–N5	104.5(3)
N7–C19	1.438(10)	N3–Ru–N6	98.4(3)
N7–C22	1.413(10)	N4–Ru–N5	78.5(3)
N7–C28	1.461(10)	N4–Ru–N6	157.8(2)
N8–C50	1.390(10)	N5–Ru–N6	79.3(3)
N8–C53	1.406(10)	C19–N7–C22	120.0(7)
N8–C59	1.455(11)	C19–N7–C28	122.2(7)
N1–Ru–N2	78.9(3)	C22–N7–C28	117.8(6)
N1–Ru–N3	157.4(2)	C50–N8–C53	120.8(7)
N1–Ru–N4	93.4(2)	C50–N8–C59	120.4(7)
N1–Ru–N5	97.9(3)	C53–N8–C59	117.8(6)
N1–Ru–N6	88.9(3)		

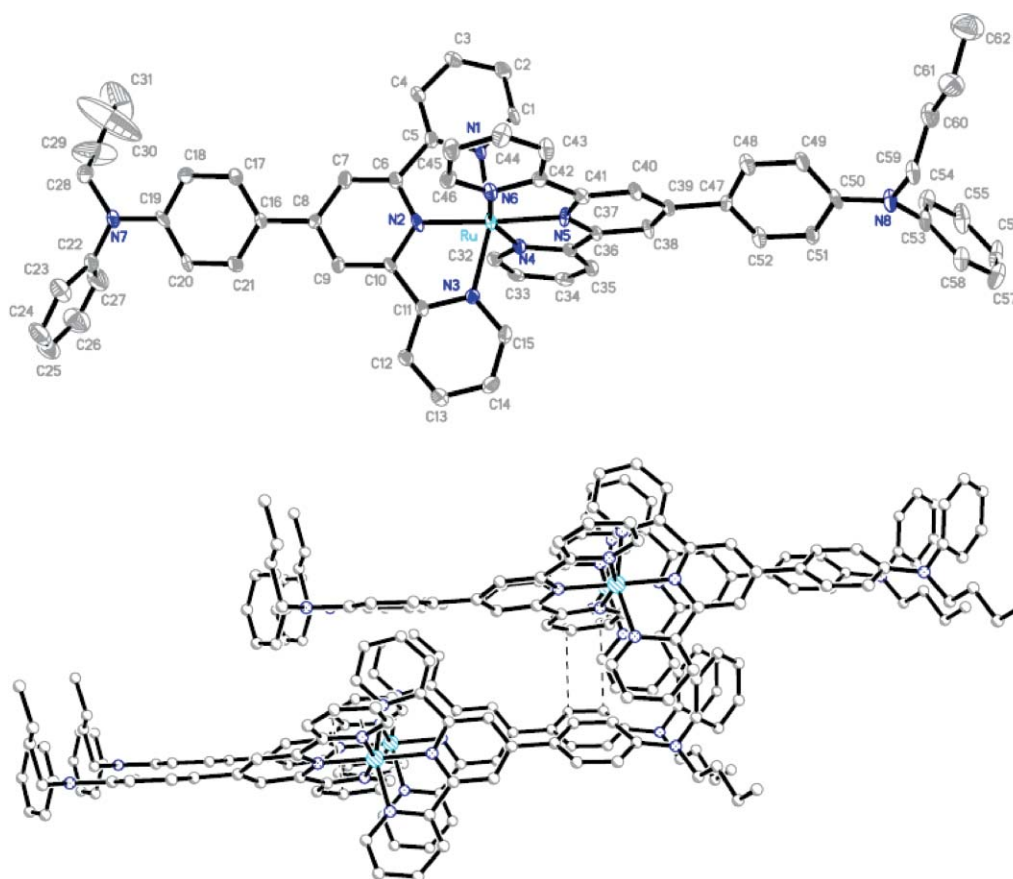


Fig. 3 ORTEP representation (top) and crystal packing (bottom) of the $[\text{Ru}(\text{L}^{13})_2](\text{PF}_6)_2$ complex (30% thermal ellipsoids); hydrogen atoms and PF_6^- anion have been omitted for clarity.

$\text{C}14\text{--}\text{C}51''$, 3.64 Å) exist between another terminal pyridyl ring and the 4-position phenyl ring from the third cation of a different column. The above facts suggest that strong conjugation exists in the oligoaniline-functionalized Ru(II) complexes in the solid state.

Thermal gravimetric analysis (TGA)

The reduced state mono- or dinuclear complexes were obtained by thermolysis of the BOC-substituted precursors under an inert atmosphere at 185 °C for 12 h. In order to prove the cleavage of the BOC substituents, we conducted TGA measurements. The TGA data of the BOC-substituted mono- or dinuclear complexes are listed in Table 2. The BOC-substituted complexes start to lose weight at 174–205 °C, according to the deprotection of the BOC substituents. For each complex, the total weight loss in the first step is basically consistent with the theoretical loss. It suggests that the removal of the BOC groups is essentially quantitative, affording oligoaniline units in the LEB form. The TGA data also indicate that the resulting complexes are stable up to around 400 °C.

Electronic absorption spectroscopy

General remarks. The absorption maxima and molar extinction coefficients of the absorption bands of ligands $\text{L}^1\text{--}\text{L}^{14}$ in DMF solutions are listed in Table 3. All ligands display two intense UV absorption bands except for the BOC-protected ligands.

Table 2 TGA Data of the BOC-substituted Ru(II) complexes (PF_6^- anion have been omitted for clarity)

Complex	T_1 [°C] ^a	Loss [%] (theoretical)	T_2 [°C] ^b
$[\text{Ru}(\text{L}^7)_2]^{2+}$	199	12.6(14.4)	414
$[\text{Ru}(\text{L}^8)_2]^{2+}$	197	21.5(22.6)	427
$[\text{Ru}(\text{L}^9)_2]^{2+}$	184	28.6(27.8)	413
$[\text{Ru}(\text{L}^{10})_2]^{2+}$	205	32.0(31.5)	414
$[(\text{PTPY})\text{Ru}(\text{L}^{11})\text{Ru}(\text{PTPY})]^{4+}$	174	8.8(8.6)	423
$[(\text{PTPY})\text{Ru}(\text{L}^{12})\text{Ru}(\text{PTPY})]^{4+}$	175	15.2(14.8)	393

^a T_1 : the start temperature for losing the BOC protected group; ^b T_2 : the decomposition temperature of the resulting complex.

The shorter-wavelength peak (279–332 nm, $\log \epsilon = 4.41\text{--}4.75$) is ascribed to the $\pi\text{--}\pi^*$ transition in the polypyridine ring. In the arrays of $\text{L}^1\text{--}\text{L}^4$ [Fig. 4 (top)] and $\text{L}^{13}\text{--}\text{L}^{14}$, the longer-wavelength peak (357–385 nm, $\log \epsilon = 4.41\text{--}4.64$) gradually red-shifts with increasing oligoaniline length, suggesting substitution with the oligoaniline donor group results in a strong shift of the $\pi\text{--}\pi^*$ transitions to lower energy.²⁴ Compared to the mono-topic ligands, the bis-topic ligands L^5 and L^6 [Fig. 4 (top)] show an opposite trend, which is probably determined by the total effect of the molecular conjugation and the molecular configuration in solution. With strong electron-withdrawing groups, the BOC-substituted ligands display only one distinct absorption band (279–288 nm, $\log \epsilon = 4.41\text{--}4.92$) due to the blue-shifted

Table 3 UV data of the ligands and complexes (PF_6^- anions have been omitted for clarity)

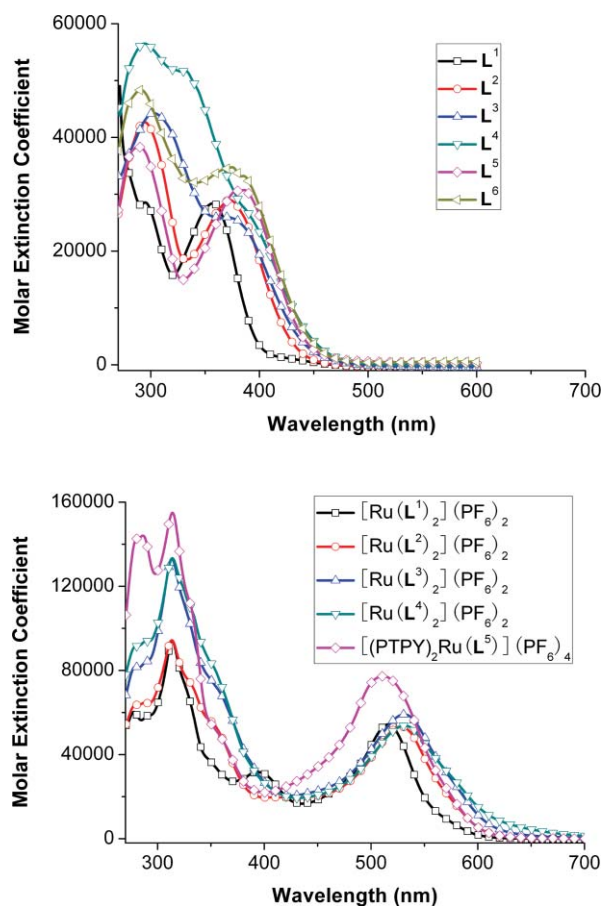
Compound	λ_{max} [nm] ($\epsilon \times 10^{-4} [\text{M}^{-1} \text{cm}^{-1}]$) ^{b, c}	
	¹ MLCT	Ligand-based
L ¹		357(2.8), 295(2.9)
L ²		373(2.9), 294(4.3)
L ³		371(2.6), 303(4.4)
L ⁴		385(sh, 2.9), 332(5.3), 294(5.6)
L ⁵		386(3.1), 289(3.4)
L ⁶		375(3.5), 291(4.8)
L ⁷		288(2.6)
L ⁸		285(3.5)
L ⁹		279(4.7)
L ¹⁰		279(5.9)
L ¹¹		287(5.3)
L ¹²		283(8.4)
L ¹³		357(4.4), 291(4.5)
L ¹⁴		363(3.1), 294(4.0)
[Ru(TPY) ₂] ²⁺ ^a	474(1.0)	
[Ru(L ¹) ₂] ²⁺	516(5.4)	394(3.2), 344(sh, 4.0), 314(9.4), 278(6.0)
[Ru(L ²) ₂] ²⁺	528(5.3)	348(sh, 5.7), 313(9.4), 280(6.4)
[Ru(L ³) ₂] ²⁺	531(5.9)	348(sh, 7.7), 313(13.3), 279(8.2)
[Ru(L ⁴) ₂] ²⁺	531(5.4)	350(sh, 8.4), 314(13.3), 279(9.1)
[(PTPY)Ru(L ⁵)Ru(PTPY)] ⁴⁺	511(7.7)	348(sh, 5.6), 314(15.5), 286(14.4)
[Ru(L ⁷) ₂] ²⁺	500(4.0)	330(sh, 7.0), 315(8.4), 289(4.9)
[Ru(L ⁸) ₂] ²⁺	498(3.9)	332(sh, 6.7), 315(8.1), 288(6.1)
[Ru(L ⁹) ₂] ²⁺	498(3.8)	333(sh, 6.5), 315(8.0), 278(7.3)
[Ru(L ¹⁰) ₂] ²⁺	498(4.3)	333(sh, 7.3), 315(8.9), 278(10.0)
[(PTPY)Ru(L ¹¹)Ru(PTPY)] ⁴⁺	496(6.6)	330(sh, 11.0), 315(14.4), 288(14.9)
[(PTPY)Ru(L ¹²)Ru(PTPY)] ⁴⁺	496(7.0)	334(sh, 10.8), 315(15.7), 288(15.5)
[Ru(L ¹³) ₂] ²⁺	529(5.6)	417(2.0), 342(sh, 4.0), 311(9.7), 276(5.3)
[Ru(L ¹⁴) ₂] ²⁺	538(5.3)	344(sh, 4.2), 311(10.1), 276(5.2)

^a Ref. [25]; ^b solvent: DMF; ^c concentration: 10^{-5} M.

longer-wavelength absorption overlapping with the shorter-wavelength band (see Fig. S4 in the ESI†).

The maxima and molar extinction coefficients of the absorption bands for all complexes in DMF solutions are also listed in Table 3. Each of the complexes displays intense UV absorption bands (276–417 nm, $\log \epsilon = 4.30$ –5.20), which are ascribed to ligand-centred (¹LC) transitions from coordinated TPY units, and a less intense band in the visible region (496–538 nm, $\log \epsilon = 4.58$ –4.89), which is attributed to the spin-allowed $d\pi(\text{M}) \rightarrow \pi^*(\text{L})$, metal-to-ligand charge-transfer transition (¹MLCT).

The MLCT absorption bands of all complexes in this work are considerably red-shifted ($\Delta\lambda_{\text{max}} = 22$ –64 nm) compared with those of $[\text{Ru}(\text{TPY})_2]^{2+}$.²⁵ The phenomenon suggests oligoanilines act as good donors in these complexes.^{23a} In the array of the mononuclear ruthenium complexes, the MLCT maximum is convergent to 531 nm with the increasing chain length in oligoaniline [Fig. 4 (bottom)]. Owing to the electron-withdrawing effect, the bathochromic effect of the BOC-substituted complexes is smaller than that of the reduced state and Bu-substituted complexes (see Fig. S4 in the ESI†). From the absorption data in Table 3, we also find that the MLCT bands are displaced towards the shorter

**Fig. 4** UV-vis spectra of the ligands (top) and complexes (bottom) in the LEB form in DMF solutions.

wavelength regions on passing from the mononuclear complexes to the dinuclear ones. This indicates that the ¹MLCT energy level of the dinuclear complex is higher than that of the mononuclear complex. Another most striking feature of the MLCT transitions in $[\text{Ru}(\text{L}^x)_2]^{2+}$ ($x = 1$ –4 and 13, 14) complexes is the significant increase in intensity (around 4–6 times compared to $[\text{Ru}(\text{TPY})_2]^{2+}$). The modification with oligoanilines in these complexes gives an unexpected $\epsilon > 50,000 \text{ cm}^3 \text{ mol}^{-1} \text{ cm}^{-1}$, the largest value observed, to our knowledge, for this type of transition in pseudo-octahedral Ru(II) complexes. The origin of this effect is associated with a mix of MLCT with the ¹ $\pi\pi^*$ excited state.²⁴ As expected, the molar absorption coefficient of the MLCT transition in the dinuclear complexes approximately doubles, compared to that in the mononuclear complexes.

Effect of oxidant and dopant. Oxidation of the pale yellow solution of L³ [Fig. 5 (a)] by silver(I) oxide results in a blue–purple solution with hypsochromic shifts of the two waves in the UV region and the growth of a broad absorption band at 562 nm, which is attributed to the characteristic electronic transition related to quinoid and benzenoid units (the EB state), *i.e.* the π_b – π_q transition.^{26,27} The addition of a drop of hydrochloric acid (a large excess) to the above solution produces a greenish yellow color. Protonation causes the shorter-wavelength absorption band to split. The longer-wavelength absorption band at 562 nm is broadened and its maximum is red-shifted to 797 nm. And two new bands at 424 and 1047 nm, respectively, are observed which

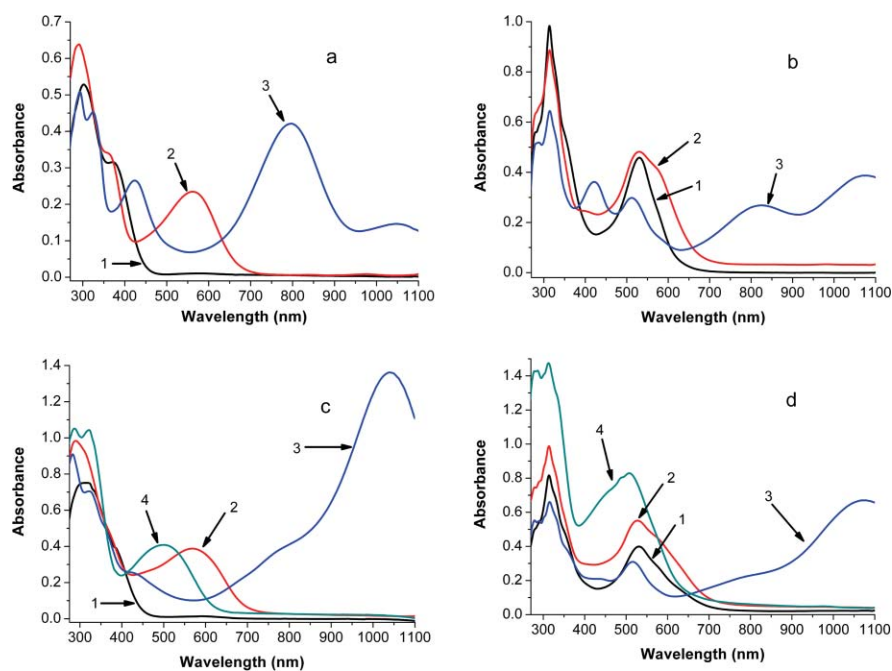


Fig. 5 Influence of oxidant and dopant on the UV-vis-NIR spectra of the ligands and complexes in DMF solutions. (a) L^3 ; (b) $[Ru(L^3)_2](PF_6)_2$; (c) L^4 ; (d) $[Ru(L^4)_2](PF_6)_2$: the LEB state (1); the EB state (2); the doped state (3); the PNB state (4).

are attributed to the polaron absorption in aniline oligomers or polymers.^{17,28}

During oxidation of ligand L^4 [Fig. 5 (c)], initial formation of the π_b - π_q transition band at 569 nm is observed. With further oxidation, the solution color turns to pink. The absorption peak at 569 nm considerably blue-shifts to 500 nm ($\Delta\lambda_{\max} = 69$ nm). The strongly hypsochromic effect reflects the decreased charge-transfer absorption in the PNB state.¹⁵ Protonation of the EB form of L^4 causes similar changes to those of L^3 , besides the absorbance in the near-IR region becomes much more intense with a definite maximum at 1039 nm. The intensity of this band is usually regarded to be directly proportional to the conductivity of polyaniline,^{27,28} suggesting the doped state of L^4 is more conductive than that of L^3 .

The changes in the UV-vis-NIR spectra of complexes $[Ru(L^3)_2](PF_6)_2$ [Fig. 5 (b)] and $[Ru(L^4)_2](PF_6)_2$ [Fig. 5 (d)], arising from oxidation and the doping effect, are essentially identical to those of the free ligands L^3 and L^4 respectively. Owing to overlap with the MLCT band, the characteristic wave of the EB or PNB state is just shown as a shoulder peak for each of them. Protonation leads the MLCT band to blue-shift and decrease in intensity, suggesting the higher $\pi^*(L)$ energy in the doped state decreases the blending degree of the MLCT and $^1\pi\pi^*$ excited states. The effects of oxidant and dopant on other ligands and complexes are shown in Fig. S5 in the ESI.†

Electrochemistry

Cyclic voltammetry (CV) has been widely used to characterize the electrochemical properties of poly- or oligoanilines, affording valuable insights into the electronic structures of the oxidized states.²⁹ Electrochemical data of the ligands are listed in Table 4. Because the redox potentials of the TPy moiety are beyond the

Table 4 Oxidation potentials (E_p in V vs Fc^+/Fc) of the ligands in CV spectra

Ligand	$E_{p,ox}^c$	Ligand	$E_{p,ox}^c$
L^1	+0.48 ^a	L^8	+1.02 ^b
L^2	+0.08 ^a	L^9	+1.07 ^b
L^3	-0.08, +0.41 ^a	L^{10}	+1.06 ^b
L^4	-0.17(sh), -0.08, +0.12 ^a	L^{11}	+1.01 ^b
L^5	+0.08 ^a	L^{12}	+1.03 ^b
L^6	-0.08, +0.24 ^a	L^{13}	+0.64 ^b
L^7	+1.21 ^b	L^{14}	+0.02, +0.55 ^b

^a DMF solvent; ^b DCM solvent; ^c concentration: 10^{-3} M; supporting electrolyte: 0.1 M nBu_4NClO_4 .

electrochemical window of the used solvents, just the oligoaniline-based oxidation waves were observed. From the data in Table 4, ligand L^1 shows a single oxidation peak at +0.48 V (vs Fc^+/Fc), in accordance with forming a radical cation species.³⁰ Similar to the voltammetric behavior of the tri-aniline analogue,³¹ two oxidation waves with basically equal amplitude are observed at -0.08 V and +0.41 V (vs Fc^+/Fc) for L^3 in this study, attributed to the formation of the benzoquinoid dication. For L^2 , L^4 , L^5 or L^6 , including even-numbered oligoaniline units, the electron transfer prefers to occur in pairs. Like the oxidation behavior of N,N' -diphenyl-*p*-phenylenediamine in an aqueous electrolyte (pH 2.5),³² a combined two-electron transfer process is observed for L^2 and L^5 , respectively, in accordance with the formation of the quinoid structure. The phenyl-capped aniline tetramer³³ and polyaniline³⁴ usually show two two-electron transfer processes, in which the first wave is assigned to a two-electron transfer process to form the di(cation radical) tetraamine (the EB state) and the second is attributed to another two-electron transfer process followed by a four-proton loss to form the PNB structure. Ligand L^6 exhibits the above similar behavior with two oxidation waves at -0.08 and

Table 5 Electrochemical data (E_p in V vs Fc^+/Fc) of the Ru(II) complexes. (All complexes were used as hexafluorophosphate salts and PF_6^- anions have been omitted for clarity)

Complex	CV		
	$E_{p,ox}$		$E_{p,red}$
	Metal-based	Oligoaniline-based	Ligand-based
$[Ru(TPY)_2]^{2+ a}$	+0.92 ^d		-1.67 ^d
$[Ru(L^1)_2]^{2+ b}$	+0.95	+0.59	-1.73, -1.96, -2.47
$[Ru(L^2)_2]^{2+ b}$	+0.84	+0.09	-1.76, -1.97, -2.45, -2.80 ^f
$[Ru(L^3)_2]^{2+ b}$	+0.91	-0.04, +0.50	-1.70, -1.92, -2.39, -2.80 ^f
$[Ru(L^4)_2]^{2+ b}$	+0.84	-0.17, +0.01, +0.24	-1.70, -1.90, -2.47
$[(PTPY)Ru(L^5)Ru(PTPY)]^{4+ b}$	+0.83	+0.16	-1.71, -1.96, -2.42, -2.74
$[Ru(L^7)_2]^{2+ c}$	+0.84 ^d	+0.64	-1.63 ^d , -1.93
$[Ru(L^8)_2]^{2+ c}$	+0.85 ^d	+1.06, +1.30	-1.61 ^d , -1.89
$[Ru(L^9)_2]^{2+ c}$	+0.83 ^d	+1.18	-1.62 ^d , -1.90
$[Ru(L^{10})_2]^{2+ c}$	- ^e	+1.13	-1.62 ^d , -1.91
$[(PTPY)Ru(L^{11})Ru(PTPY)]^{4+ c}$	+0.84 ^d	+1.09	-1.63 ^d , -1.89
$[(PTPY)Ru(L^{12})Ru(PTPY)]^{4+ c}$	+0.85 ^d	+1.12	-1.63 ^d , -1.90
$[Ru(L^{13})_2]^{2+ c}$	+0.89 ^d	+0.58	-1.69 ^d , -1.96
$[Ru(L^{14})_2]^{2+ c}$	+0.90 ^d	+0.09, +0.51	-1.69 ^d , -1.92

^a Ref. [25]; ^b DMF solvent; ^c CH_3CN solvent; ^d reversible, values calculated as averages of the cathodic and anodic peaks; ^e overlapped; ^f shoulder peak.

+0.24 V (vs Fc^+/Fc), while three oxidation waves at -0.17 (sh), -0.08 and +0.12 V (vs Fc^+/Fc) are observed for L^4 , arising from the distinct splitting of the first two-electron transfer processes. The difference should be attributed to the unsymmetric structure formed by the TPY moiety on one end in L^4 . The second oxidative wave in L^6 is apparently higher than that in L^4 , suggesting the oxidation of the EB state to the PNB state in L^6 is more difficult.

Compared with those of ligands L^{1-6} , the oligoaniline-based oxidation waves of ligands L^{7-12} are markedly shifted to positive potentials due to the strong electron-withdrawing ability of the BOC substituents. L^{13} shows a single oxidation peak at +0.64 V (vs Fc^+/Fc), in accordance with forming a radical cation species, while L^{14} displays two oxidation peaks at +0.02 and +0.55 V (vs Fc^+/Fc), relative to the formation of di(cation radical) species.³⁵

Besides the oligoaniline-based oxidation waves as mentioned above, each complex shows the voltammetric responses expected for the $[Ru(TPY)_2]^{2+}$ core, typically $Ru^{3+/2+}$ couple, and two terpyridyl-centred reduction processes {the $[Ru(TPY)_2]^{2+}/[Ru(TPY)(TPY^-)]^+$ and $[Ru(TPY)(TPY^-)]^+/[Ru(TPY^-)]^0$ couples at approximately -1.7 and -1.9 V respectively}. The voltammetric responses for the $[Ru(TPY)_2]^{2+}$ core are relatively well known²³ and, rather than give a detailed description, assignments are summarized in Table 5. However, introduction of the oligoaniline unit in each of $[Ru(L^{1-4})_2]^{2+}$ and $[(PTPY)Ru(L^5)Ru(PTPY)]^{4+}$ lowers the reversibility of the redox waves for the $[Ru(TPY)_2]^{2+}$ core, and extra reduction processes at more negative potentials are present. Similar phenomena are observed in the analogue of monomeric³⁶ or dimeric³⁷ Ru(II) complexes with an amine donor group.

Compared with those in free ligands, the oligoaniline-based oxidation waves in most of the complexes shift to more positive potentials. For example, the third oxidative wave in L^4 is present at +0.12 V (vs Fc^+/Fc), while the counterpart in $[Ru(L^4)_2](PF_6)_2$ is observed at +0.24 V (vs Fc^+/Fc). The significant shift ($\Delta E_p = 0.12$ V) reflects the phenyl-capped aniline tetramer in the latter is more difficult to be fully oxidized to the PNB form, arising from the interaction between the oligoaniline unit and the $[Ru(TPY)_2]^{2+}$ core. The substituent effect on the oligoaniline-based oxidation in complexes is similar to that in ligands, typically shown in

Fig. 6. The metal-centred oxidation potentials slightly shift to the negative direction, while the terpyridyl-centred reduction waves show the reverse tendency in the BOC-substituted complexes.

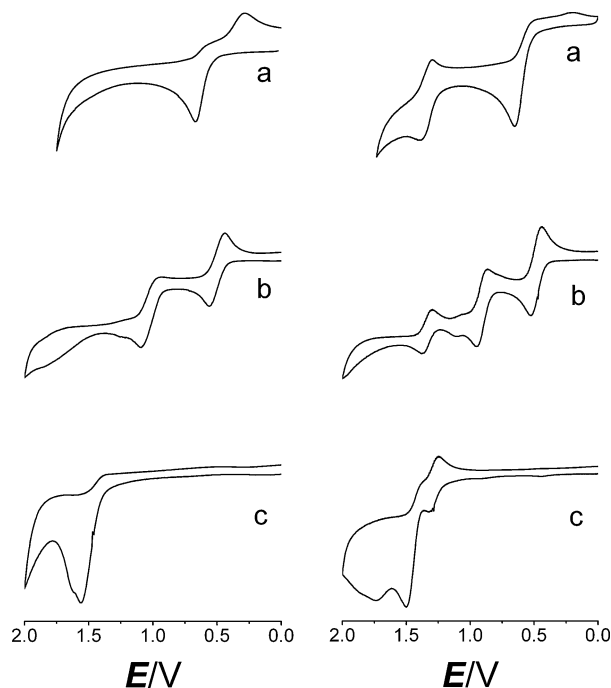


Fig. 6 Substituent effect (R) on the oxidation behavior of aniline dimer in ligands and complexes. (a) R = -H (L^2 (left) and $[Ru(L^2)_2](PF_6)_2$ (right)); (b) R = -Bu (L^4 (left) and $[Ru(L^4)_2](PF_6)_2$ (right)); (c) R = -BOC (L^8 (left) and $[Ru(L^8)_2](PF_6)_2$ (right)).

Like other reported binuclear Ru^{2+} complexes linearly arranged with π -conjugated organic oligomers as spacers,^{18b,38} each of the obtained binuclear complexes, such as $[(PTPY)Ru(L^5)Ru(PTPY)](PF_6)_2$, $[(PTPY)Ru(L^{11})Ru(PTPY)](PF_6)_2$ and $[(PTPY)Ru(L^{12})Ru(PTPY)](PF_6)_2$, shows a single-wave for the

Table 6 Energy levels and E_g of the Ru(II) complexes. (All complexes were used as hexafluorophosphate salts and PF_6^- anions have been omitted for clarity)

Complex	HOMO ^a (eV)	LUMO ^a (eV)	E_g (eV)
$[\text{Ru}(\text{L}^1)_2]^{2+,b}$	5.22	3.17	2.05
$[\text{Ru}(\text{L}^2)_2]^{2+,b}$	4.77	3.15	1.62
$[\text{Ru}(\text{L}^3)_2]^{2+,b}$	4.61	3.22	1.39
$[\text{Ru}(\text{L}^4)_2]^{2+,b}$	4.51	3.15	1.36
$[(\text{PTPY})\text{Ru}(\text{L}^5)\text{Ru}(\text{PTPY})]^{4+,b}$	4.84	3.20	1.64
$[\text{Ru}(\text{L}^7)_2]^{2+,c}$	5.31	3.23	2.08
$[\text{Ru}(\text{L}^8)_2]^{2+,c}$	5.56	3.25	2.31
$[\text{Ru}(\text{L}^9)_2]^{2+,c}$	5.57	3.24	2.33
$[\text{Ru}(\text{L}^{10})_2]^{2+,c}$	5.58	3.25	2.33
$[(\text{PTPY})\text{Ru}(\text{L}^{11})\text{Ru}(\text{PTPY})]^{4+,c}$	5.56	3.24	2.32
$[(\text{PTPY})\text{Ru}(\text{L}^{12})\text{Ru}(\text{PTPY})]^{4+,c}$	5.57	3.23	2.34
$[\text{Ru}(\text{L}^{13})_2]^{2+,c}$	5.29	3.19	2.10
$[\text{Ru}(\text{L}^{14})_2]^{2+,c}$	4.78	3.18	1.60

^a $\text{HOMO} = \{4.8 + [E_{\text{ox,onset}} - E_{1/2}(\text{Fc}^+/\text{Fc})]\}$ (eV); $\text{LUMO} = \{4.8 + [E_{\text{red,onset}} - E_{1/2}(\text{Fc}^+/\text{Fc})]\}$ (eV), where $E_{1/2}(\text{Fc}^+/\text{Fc}) = (E_{\text{pa}} + E_{\text{pc}})/2$, $E_{\text{ox,onset}}$ and $E_{\text{red,onset}}$ were calculated from the onset value of the first oxidation wave in the anodic segment and the first reduction wave in the cathodic segment of the CV spectrum respectively; ^b DMF solvent; ^c CH_3CN solvent.

$\text{Ru}^{3+}/\text{Ru}^{2+}$ couple, which might indicate that the electronic coupling between the two Ru^{2+} centers is comparatively weak.

The HOMO-LUMO gaps (E_g) of Ru(II) complexes, calculated from the electrochemical measurements,³⁹ are listed in Table 6. For unsubstituted and Bu-substituted oligoaniline functionalized Ru(II) complexes, the E_g values gradually decrease with increasing chain length of oligoaniline unit, arising from the decrease of the HOMO level but with no change in the LUMO level. With the introduction of a strong electron-withdrawing substituent (BOC), the E_g value considerably increases. But in the BOC-substituted series it is essentially unchanged. The dinuclear Ru(II) complexes possess slightly larger gaps than the corresponding mononuclear ones. These results are well in line with those of the spectroscopic studies.

Oxidative electropolymerization

With incorporation of the diphenylamine unit in the terpyridine ligand, complexes $[\text{Ru}(\text{L}^1)_2](\text{PF}_6)_2$, $[\text{Ru}(\text{L}^7)_2](\text{PF}_6)_2$ and $[\text{Ru}(\text{L}^{13})_2](\text{PF}_6)_2$ display interesting electro-polymerization behaviours. Continuous cycling of the working Pt or ITO electrode potential from 0 to 1.8 V in a CH_3CN solution containing 0.5 mmol cm^{-3} $[\text{Ru}(\text{L}^{13})_2](\text{PF}_6)_2$ resulted in the formation of a red adherent film on the electrode surface. A wave at +1.02 V (*vs* SCE) is observed in the first oxidation segment [Fig. 7 (a)]. As the cyclic scan proceeds, it gradually shifts to positive potentials with increasing intensities and finally combines with the metal-based oxidation wave. The SEM images [Fig. 7 (b)] indicate the formation of the polymer film. Similar phenomena were also present in $[\text{Ru}(\text{L}^1)_2](\text{PF}_6)_2$ and $[\text{Ru}(\text{L}^7)_2](\text{PF}_6)_2$. It is believed that the waves at +1.17 V (*vs* SCE) for $[\text{Ru}(\text{L}^{13})_2](\text{PF}_6)_2$, +1.02 V (*vs* SCE) for $[\text{Ru}(\text{L}^{13})_2](\text{PF}_6)_2$ and +1.08 V (*vs* SCE) for $[\text{Ru}(\text{L}^7)_2](\text{PF}_6)_2$ are attributed to the formation of a radical cation species, which trigger the polymerization process, and the $[\text{Ru}(\text{TPY})]^{2+}$ cores in these complexes play a key role in the stabilization of the radical cation species.⁴⁰

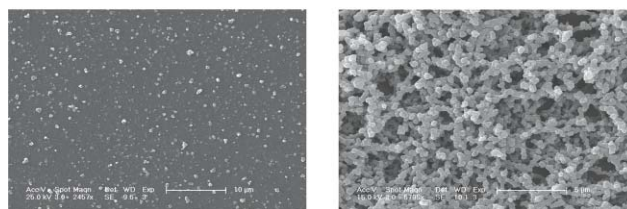
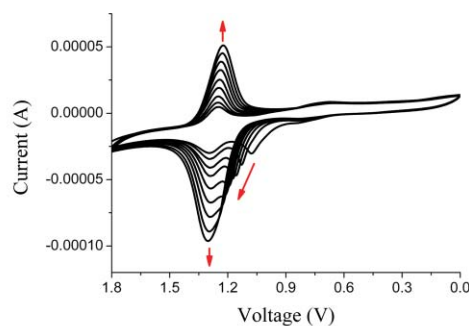


Fig. 7 Oxidative electropolymerization of $[\text{Ru}(\text{L}^{13})_2](\text{PF}_6)_2$. (a) Top: Repetitive cyclic voltammograms on a Pt electrode; (b) Bottom: SEM images of poly- $[\text{Ru}(\text{L}^{13})_2]^{2+}$ -coated ITO after 20 segments (left) and 100 segments (right).

Experimental

General

Melting points were recorded on a hot stage apparatus and are uncorrected. ^1H and ^{13}C NMR spectra were recorded on Bruker AV 300 spectrometers and referenced with respect to TMS internal standard. Elemental analyses were carried out using a Bio-Rad Co's elemental analytical instrument. UV-Vis spectra were obtained using a Perkin-Elmer UV-35 spectrophotometer. PL spectra were performed on a Perkin-Elmer LS50B spectrometer. CV measurements were conducted on a EG & 283 electrochemical workstation with a three-electrode electrochemical cell using SCE or AgCl/Ag and Pt wire as the reference and counter electrode, respectively. $n\text{-Bu}_4\text{NClO}_4$ (0.1 mol cm^{-3}) was used as the supporting electrolyte. The scan rate was 100 mV s^{-1} . Thermal analyses were carried out in a nitrogen atmosphere with a heating rate of $10 \text{ }^\circ\text{C min}^{-1}$ on a thermal gravimetric analysis (TGA) Perkin-Elmer 7 series instrument.

Reactions under an argon atmosphere were carried out in oven-dried glassware using standard Schlenk techniques. Tetrahydrofuran (THF) was distilled under argon from sodium benzophenone ketyl. Toluene was distilled under argon from molten sodium. *N,N*-Dimethylformamide (DMF) was treated with 5 \AA molecular sieves and distilled under reduced pressure. All other solvents were analytical reagent grades and used as supplied.

All the reagents were analytical grades. 1,4-Phenylenediamine was sublimed while aniline was distilled before use. *p*-Amino-diphenylamine, benzophenone, palladium acetate ($\text{Pd}(\text{OAc})_2$), sodium *tert*-butoxide (NaOBu^t) (Acros), bis[2-diphenylphosphino]phenyl]ether (DPEphos) (Acros), di-*tert*-butyl bicarbonate ((BOC)₂O) (Acros), 4-(dimethylamino)pyridine (4-DMAP) (Acros), palladium on carbon (Pd/C , 10%), ammonium formate, 2-acetylpyridine, 4-bromo-phenylaldehyde, NaH (>52%, in mineral oil), *n*-bromobutylane were all used as received without further purification.

4'-(4-Bromophenyl)-2,2':6',2''-terpyridine (**10**), 4'-phenyl-2,2':6',2''-terpyridine (PTPY),²² *N*-diphenylmethylene-4-bromoaniline (**5**),¹⁵ *N*-(diphenylmethylene-*N'*-(*tert*-butoxycarbonyl)-*N'*-(4-bromophenyl)-*p*-phenylenediamine (**2**), *N*-(diphenylmethylene-*N'*-(*tert*-butoxycarbonyl)-*N'*-(phenyl)-*p*-phenylenediamine (**3**), *N*-(diphenylmethylene-*N'*-(*tert*-butoxycarbonyl)-*N'*-[4-(*N*-*tert*-butoxycarbonylanilino)]phenyl-*p*-phenylenediamine (**6**) and compound **8**¹⁹ were synthesized according to literature methods.

Preparations

The ligand L⁷. 4'-(4-Bromophenyl)-2,2':6',2''-terpyridine (**10**) (3.88 g, 10 mmol), Pd(OAc)₂ (15.0 mg, 0.067 mmol) and DPEphos (49.0 mg, 0.091 mmol) were charged into a flask and purged with argon. Aniline (1.2 cm³, 13 mmol) was added *via* syringe, followed by toluene (30 cm³). NaOBu^t (1.63 g, 17 mmol) was added in one portion. The reaction mixture was heated to 80 °C with stirring for 3–4 h (as monitored by thin layer chromatography). The solvent was removed by rotary evaporation. The residue was dissolved in dichloromethane, washed with distilled water, dried over anhydrous sodium sulfate and concentrated.

The residue was dissolved in THF (80 cm³), and (BOC)₂O (1M in THF) (15 cm³, 15.0 mmol) and 4-DMAP (0.15 g, 1.2 mmol) were added. The reaction mixture was refluxed for 24 h and cooled to room temperature and concentrated. The residue was separated by column chromatography [Al₂O₃, PE/DCM = 5:1 (V/V) containing 5% (V) triethylamine]. Product **L⁷** was obtained as a white powder. (4.2 g, 84%); mp 166 °C; Found: C, 76.87; H, 5.50; N, 10.85. Calc. for C₃₂H₂₈N₄O₂: C, 76.78; H, 5.64; N, 11.19%; ¹H NMR (300 MHz, DMSO-*d*₆): δ 8.75 (d, J = 4.5 Hz, 2 H; H^{6,6'}, terpy), 8.68 (s, 2 H; H^{3',5'}, terpy), 8.65 (d, J = 7.8 Hz, 2 H; H^{3,3'}, terpy), 8.02 (t, J = 7.7 Hz, 2 H; H^{4,4'}, terpy), 7.89 (d, J = 8.4 Hz, 2 H), 7.51 (t, J = 6.9 Hz, 2 H; H^{5,5'}, terpy), 7.43–7.37 (m, 4 H), 7.28–7.21 (m, 3 H; Ar), 1.47 (s, 9 H, -OC(CH₃)₃); ¹³C NMR (75 MHz, CDCl₃): δ 156.6, 156.4, 154.0 (–C=O), 150.0, 149.5, 144.4, 143.2, 137.2, 135.9, 129.3, 128.0, 127.5, 127.4, 126.3, 124.2, 121.8, 119.1, 81.9 (–OC(CH₃)₃), 28.7 (–CH₃).

L⁸. Compound **3** (12.0 g, 26.8 mmol), ammonium formate (25.0 g, 396.5 mmol), and palladium on carbon (10%) (2.3 g, 1.1 mmol) were charged into a round-bottomed flask and purged with argon. THF (50 cm³) and methanol (125 cm³) were added, and the reaction mixture was refluxed until conversion to amine **4** was complete (as monitored by thin layer chromatography). The reaction mixture was cooled to room temperature and concentrated. The residue was dissolved in dichloromethane, filtered through Celite, and then concentrated. The solid was washed with hexanes and filtered. The white powder was dried in vacuum at 50 °C for 24 h. Yield of product **4** was 7.5 g (98%).

Compound **4** (3.41 g, 12 mmol), Pd(OAc)₂ (16.2 mg, 0.072 mmol) and DPEphos (62.9 mg, 0.117 mmol) were charged into a flask and purged with argon. Compound **10** (3.88 g, 10 mmol) was added, followed by toluene (40 cm³). The solution was warmed to 50 °C to aid dissolution. NaOBu^t (1.73 g, 18 mmol) was added in one portion. The reaction mixture was heated to 80 °C with stirring for about 5 h (as monitored by thin layer chromatography). The solvent was removed by rotary evaporation. The residue was dissolved in dichloromethane, washed with distilled water, dried over anhydrous sodium sulfate and concentrated. The obtained solid was dissolved in THF

(50 cm³), and (BOC)₂O (1M in THF) (16 cm³, 16.0 mmol) and 4-DMAP (0.18 g, 1.5 mmol) were added. The reaction mixture was refluxed for 24 h. The solvent was removed, and **L⁸** was separated by column chromatography [Al₂O₃, PE/DCM = 5:1 (V/V) containing 5% (V) triethylamine] as white powder. (6.1 g, 88%); mp 190 °C; Found: C, 74.94; H, 6.00; N, 9.78. Calc. for C₄₃H₄₁N₅O₄: C, 74.65; H, 5.97; N, 10.12%; ¹H NMR (300 MHz, DMSO-*d*₆): δ 8.76 (d, J = 4.0 Hz, 2 H; H^{6,6'}, terpy), 8.70 (s, 2 H; H^{3',5'}, terpy), 8.67 (d, J = 7.9 Hz, 2 H; H^{3,3'}, terpy), 8.04 (t, J = 7.7 Hz, 2 H; H^{4,4'}, terpy), 7.93 (d, J = 8.6 Hz, 2 H), 7.53 (t, J = 7.0 Hz, 2 H; H^{5,5'}, terpy), 7.42–7.34 (m, 4 H), 7.24–7.20 (m, 7 H; Ar), 1.42 (s, 9 H, -OC(CH₃)₃), 1.38 (s, 9 H, -OC(CH₃)₃); ¹³C NMR (75 MHz, CDCl₃): δ 156.6, 156.4, 154.1 (–C=O), 154.0 (–C=O), 149.5, 144.1, 143.2, 141.0, 140.5, 137.3, 136.1, 129.2, 128.1, 127.5, 126.2, 124.2, 121.8, 119.1, 82.0 (–OC(CH₃)₃), 81.7 (–OC(CH₃)₃), 28.6 (–CH₃).

L⁹ and **L¹⁰** were prepared by the same procedures besides using compound **6** and **8** as starting materials and using THF instead of toluene as solvent.

L⁹. obtained as white solid in 76% yield. mp 195 °C; Found: C, 73.47; H, 6.18; N, 9.13. Calc. for C₃₄H₃₄N₆O₆: C, 73.45; H, 6.16; N, 9.52%; ¹H NMR (300 MHz, DMSO-*d*₆): δ 8.76 (d, J = 4.2 Hz, 2 H; H^{6,6'}, terpy), 8.70 (s, 2 H; H^{3',5'}, terpy), 8.67 (d, J = 8.0 Hz, 2 H; H^{3,3'}, terpy), 8.04 (t, J = 7.7 Hz, 2 H; H^{4,4'}, terpy), 7.91 (d, J = 8.6 Hz, 2 H), 7.53 (t, J = 4.9 Hz, 2 H; H^{5,5'}, terpy), 7.41–7.32 (m, 4 H), 7.23–7.19 (m, 11 H; Ar), 1.47 (s, 9 H, -OC(CH₃)₃), 1.42 (s, 9 H, -OC(CH₃)₃), 1.37 (s, 9 H, -OC(CH₃)₃); ¹³C NMR (75 MHz, CDCl₃): δ 156.6, 156.4, 154.2 (–C=O), 154.1 (–C=O), 154.0 (–C=O), 150.0, 149.5, 144.1, 143.2, 140.9, 140.8, 140.6, 140.5, 137.3, 136.1, 129.1, 128.1, 127.6, 127.4, 126.2, 124.2, 121.8, 119.1, 82.0 (–OC(CH₃)₃), 81.8 (–OC(CH₃)₃), 81.6 (–OC(CH₃)₃), 28.6 (–CH₃).

L¹⁰. obtained as white solid in 69% yield. mp 196 °C; Found: C, 72.88; H, 6.20; N, 8.94. Calc. for C₆₅H₆₇N₇O₈: C, 72.67; H, 6.29; N, 9.13%; ¹H NMR (300 MHz, DMSO-*d*₆): δ 8.76 (d, J = 4.0 Hz, 2 H; H^{6,6'}, terpy), 8.70 (s, 2 H; H^{3',5'}, terpy), 8.67 (d, J = 8.0 Hz, 2 H; H^{3,3'}, terpy), 8.04 (t, J = 7.6 Hz, 2 H; H^{4,4'}, terpy), 7.92 (d, J = 8.5 Hz, 2 H), 7.53 (t, J = 5.8 Hz, 2 H; H^{5,5'}, terpy), 7.40 (d, J = 8.5 Hz, 4 H), 7.32–7.16 (m, 17 H; Ar), 1.41 (s, 9 H, -OC(CH₃)₃), 1.38 (s, 9 H, -OC(CH₃)₃), 1.36 (s, 9 H, -OC(CH₃)₃), 1.36 (s, 9 H, -OC(CH₃)₃); ¹³C NMR (75 MHz, CDCl₃): δ 156.2, 156.0, 153.8 (–C=O), 153.7 (–C=O), 153.6 (–C=O), 149.6, 149.1, 143.7, 142.9, 140.5, 140.4, 140.3, 140.1, 136.9, 135.7, 128.7, 128.2, 127.7, 127.2, 127.0, 125.8, 123.8, 121.4, 118.8, 81.6 (–OC(CH₃)₃), 81.4 (–OC(CH₃)₃), 81.3 (–OC(CH₃)₃), 81.2 (–OC(CH₃)₃), 28.2 (–CH₃), 27.9 (–CH₃).

L¹¹. 1,4-Phenylenediamine (0.52 g, 4.8 mmol), 4'-(4-bromophenyl)-2,2':6',2''-terpyridine (**10**) (3.88 g, 10 mmol), Pd(OAc)₂ (15.0 mg, 0.067 mmol) and DPEphos (49.0 mg, 0.091 mmol) were charged into a flask and purged with argon. THF (40 cm³) was added *via* syringe, and the suspension was warmed to 50 °C to aid the dissolution. NaOBu^t (1.63 g, 17 mmol) was added in one portion. The reaction mixture was refluxed with stirring for 3–4 h (as monitored by thin layer chromatography). The solvent was removed by rotary evaporation. The residue was dissolved in dichloromethane, washed with distilled water, dried over anhydrous sodium sulfate and concentrated. The obtained

solid was dissolved in THF (80 cm³), and (BOC)₂O (1M in THF) (15 cm³, 15.0 mmol) and 4-DMAP (0.15 g, 1.2 mmol) were added. The reaction mixture was refluxed for 24 h. Product **L**¹¹ was separated by column chromatography [Al₂O₃, PE/DCM = 5:1 (V/V) containing 5% (V) triethylamine] as white powder. (2.7 g, 62%). mp 221 °C; Found: C, 75.25; H, 5.56; N, 11.98. Calc. for C₃₈H₅₀N₈O₄: C, 75.47; H, 5.46; N, 12.14%; ¹H NMR (300 MHz, DMSO-d₆): δ 8.76 (d, J = 4.2 Hz, 4 H; H^{6,6'}, terpy), 8.71 (s, 4 H; H^{3,5'}, terpy), 8.67 (d, J = 8.0 Hz, 4 H; H^{3,3'}, terpy), 8.03 (t, J = 4.7 Hz, 4 H; H^{4,4'}, terpy), 7.94 (d, J = 8.6 Hz, 4 H), 7.53 (t, J = 6.0 Hz, 4 H; H^{5,5'}, terpy), 7.43 (d, J = 8.5 Hz, 4 H), 7.30 (s, 4 H; Ar), 1.44 (s, 18 H, -OC(CH₃)₃); ¹³C NMR (75 MHz, DMSO-d₆): δ 156.6, 155.8, 153.9 (-C=O), 150.2, 149.5, 144.8, 141.5, 138.3, 135.7, 129.2, 128.6, 128.2, 125.4, 121.8, 118.6, 81.6 (-OC(CH₃)₃), 28.7 (-CH₃).

L¹². A solution of 1,4-phenylenediamine (**11**) (1.62 g, 15.0 mmol), bromide **5** (10.83 g, 32.2 mmol), Pd(OAc)₂ (116.4 mg, 0.52 mmol), DPEphos (514.6 mg, 0.96 mmol) and NaOBu^t (5.0 g, 52 mmol) in THF (40 cm³) was refluxed for 5 h under argon. The solution was concentrated, and the residue was dissolved in dichloromethane, washed with distilled water, dried over anhydrous sodium sulfate and concentrated. The residue was dissolved in THF (200 cm³), and (BOC)₂O (1M in THF) (50 cm³, 50.0 mmol) and 4-DMAP (0.60 g, 4.9 mmol) were added. The reaction mixture was refluxed for 24 h. The solvent was removed, and the residue was separated by column chromatography [silica gel, PE/DCM = 1:8 (V/V)]. Product **12** was obtained as yellow powder: 10.7 g (87%).

Compound **12** (3.27 g, 4.0 mmol), ammonium formate (7.0 g, 111.0 mmol), and palladium on carbon (10%) (0.85 g, 0.8 mmol) were charged into a round-bottomed flask and purged with argon. THF (100 cm³) and methanol (100 cm³) were added. The reaction mixture was refluxed until conversion to diamine **13** completely (as monitored by thin layer chromatography). The solvent was removed by rotary evaporation. The residue was dissolved in a hot mixture of isopropanol (500 cm³), CHCl₃ (100 cm³) and water (50 cm³), then allowed to stand at room temperature for 12 h. The precipitate which formed was collected by filtration, and washed with distilled water followed by isopropanol. The solid was dried under vacuum to afford the compound **13** as a white powder (1.9 g, 94%).

A solution of diamine **13** (1.53 g, 3.12 mmol), compound **10** (2.54 g, 6.54 mmol), Pd(OAc)₂ (44.0 mg, 0.20 mmol), DPEphos (158 mg, 0.29 mmol) and NaOBu^t (1.57 g, 16.35 mmol) in THF (40 cm³) and triethylamine (10 cm³) was refluxed for 48 h under argon. After this period, the heat was temporarily removed, and 4-DMAP (0.12 g, 0.98 mmol), THF (40 cm³), and a 1.0 M solution of (BOC)₂O (20.0 mmol) in THF (20 cm³) were added. The reaction mixture was refluxed for 24 h. The solvent was removed by rotary evaporation. The residue was dissolved in dichloromethane, washed with distilled water, dried over anhydrous sodium sulfate and concentrated. The solid was re-dissolved in the boiling THF (50 cm³) and was poured into hot MeOH (200 cm³) and allowed to stand for 12 h at room temperature. The precipitate formed was collected by filtration and the procedure was operated for one more time. The solid was dried under vacuum to afford a white powder (**L**¹³) (3.1 g, 76%). mp 214 °C; Found: C, 73.29; H, 5.83; N, 10.50. Calc. for C₈₀H₇₆N₁₀O₈: C, 73.60; H, 5.87; N, 10.73%; ¹H NMR

(300 MHz, DMSO-d₆): δ 8.76 (d, J = 4.1 Hz, 4 H; H^{6,6'}, terpy), 8.74 (s, 4 H; H^{3,5'}, terpy), 8.69 (d, J = 8.0 Hz, 4 H; H^{3,3'}, terpy), 7.94 – 7.87 (m, 8 H), 7.41 – 7.36 (m, 8 H), 7.22 – 7.20 (m, 12 H; Ar), 1.50 (s, 18 H, -OC(CH₃)₃), 1.48 (s, 18 H, -OC(CH₃)₃); ¹³C NMR (75 MHz, CDCl₃): δ 156.2, 155.9, 153.7 (-C=O), 153.6 (-C=O), 149.6, 149.1, 143.7, 140.4, 140.2, 136.9, 135.6, 127.7, 127.2, 127.1, 123.8, 121.4, 118.8, 81.6 (-OC(CH₃)₃), 81.4 (-OC(CH₃)₃), 28.3 (-CH₃).

L¹³. The BOC-protected ligand **L**⁷ (2.16 g, 4.3 mmol) was placed in a flask under argon. The system was heated to 185 °C for 12 h. After cooling to room temperature, THF (20 cm³) was added to dissolve the solid. NaH (0.41 g, >52% in mineral oil) was added and purged with argon. The reaction mixture was stirred for 1 h at room temperature, and then 1-bromobutylane (10 cm³, 8 mmol) was added dropwise *via* syringe. The solution was refluxed until the conversion was complete (as monitored by thin layer chromatography). The solution was cooled to room temperature and poured onto ice-water mixture, extracted with DCM until the water phase was colorless. The combined organic solutions were washed with distilled water, dried over anhydrous sodium sulfate and concentrated. The residue was separated by column chromatography [silica gel, PE/DCM = 8:1 (V/V) containing 5% (V) triethylamine]. Product **L**¹³ was obtained as white powder (1.8 g, 93%). mp 126 °C; Found: C, 81.79; H, 6.20; N, 11.98. Calc. for C₃₁H₂₈N₄: C, 81.55; H, 6.18; N, 12.27%; ¹H NMR (300 MHz, DMSO-d₆): δ 8.76 (d, J = 4.7 Hz, 2 H; H^{6,6'}, terpy), 8.68 – 8.65 (m, 4 H; H^{3,5',3,3'}, terpy), 8.03 (t, J = 8.6 Hz, 2 H; H^{4,4'}, terpy), 7.79 (d, J = 8.8 Hz, 2 H), 7.52 (t, J = 6.6 Hz, 2 H; H^{5,5'}, terpy), 7.41 (t, J = 7.8 Hz, 2 H), 7.22 (d, J = 7.6 Hz, 2 H), 7.15 (t, J = 7.3 Hz, 1 H), 6.99 (d, J = 8.8 Hz, 2 H; Ar), 3.77 (t, J = 7.5 Hz, 2 H, α(-CH₂)), 1.61 (m, 2 H, β(-CH₂)), 1.36 (m, 2 H, γ(-CH₂)), 0.90 (t, J = 7.3 Hz, 3 H, -CH₃); ¹³C NMR (75 MHz, CDCl₃): δ 156.5, 155.8, 149.9, 149.2, 149.1, 147.4, 136.8, 129.5, 128.8, 128.1, 124.0, 123.6, 123.3, 121.3, 117.9, 52.2 (α(-CH₂)), 29.7 (β(-CH₂)), 20.3 (γ(-CH₂)), 13.9 (-CH₃).

Ligand **L**¹⁴ was obtained by the same procedures except using compound **L**⁸ as the starting material.

L¹⁴. obtained as yellow solid in 92% yield. mp 143 °C; Found: C, 81.72; H, 6.54; N, 11.73. Calc. for C₄₁H₄₁N₅: C, 81.56; H, 6.84; N, 11.60%; ¹H NMR (300 MHz, DMSO-d₆): δ 8.72 (d, J = 3.9 Hz, 2 H; H^{6,6'}, terpy), 8.63 – 8.61 (m, 4 H; H^{3,5',3,3'}, terpy), 7.99 (t, J = 8.6 Hz, 2 H; H^{4,4'}, terpy), 7.74 (d, J = 8.7 Hz, 2 H), 7.48 (t, J = 6.1 Hz, 2 H; H^{5,5'}, terpy), 7.26 (t, J = 7.9 Hz, 2 H), 7.10 (d, J = 8.8 Hz, 2 H), 7.00 – 6.86 (m, 7 H; Ar), 3.65 (m, 4 H, α(-CH₂)), 1.54 (m, 4 H, β(-CH₂)), 1.34 (m, 4 H, γ(-CH₂)), 0.89 (m, 6 H, -CH₃); ¹³C NMR (75 MHz, CDCl₃): δ 156.6, 155.7, 149.9, 149.6, 149.1, 148.2, 144.7, 140.7, 136.8, 129.3, 128.0, 127.3, 126.6, 123.6, 122.4, 121.3, 120.8, 120.4, 117.7, 115.9, 52.25 (α(-CH₂)), 29.7 (β(-CH₂)), 20.3 (γ(-CH₂)), 14.0 (-CH₃).

General method for mononuclear complexes [Ru(L)₂](PF₆)₂ (L = **L**⁷, **L**⁸, **L**⁹, **L**¹⁰, **L**¹³ and **L**¹⁴)

The appropriate metal chloride (RuCl₃·3H₂O) and ligand **L** (2.1 eq.) were heated at reflux in EtOH (150 cm³) containing several drops of *N*-ethylmorpholine for 12 h. After cooling to room temperature, aqueous NH₄PF₆ was added and the precipitate was purified by column chromatography (silica gel, CH₃CN/sat.

aqueous $\text{KNO}_3/\text{H}_2\text{O}$). The major red fraction was collected and reduced to half its volume *in vacuo* and treated with aqueous NH_4PF_6 . The precipitate was collected by filtration. The solid was redissolved in CH_3CN , to which water was added until a precipitate was obtained. The precipitate was dried under vacuum to give a red solid.

$[\text{Ru}(\text{L}^7)_2](\text{PF}_6)_2$. obtained as red solid in 67% yield; Found: C, 54.95; H, 3.87; N, 8.20. Calc. for $\text{C}_{64}\text{H}_{56}\text{F}_{12}\text{N}_8\text{O}_4\text{P}_2\text{Ru}$: C, 55.21; H, 4.05; N, 8.05%; ^1H NMR (300 MHz, DMSO-d_6): δ 9.46 (s, 4 H; $\text{H}^{3',5'}$, terpy), 9.09 (d, $J = 8.2$ Hz, 4 H; $\text{H}^{3,3'}$, terpy), 8.39 (d, $J = 8.6$ Hz, 4 H), 8.07 (t, $J = 7.9$ Hz, 4 H; $\text{H}^{4,4'}$, terpy), 7.60–7.45 (m, 10 H), 7.37–7.04 (m, 12 H; Ar), 1.48 (s, 18 H, $-\text{OC}(\text{CH}_3)_3$); ^{13}C NMR (75 MHz, DMSO-d_6): δ 158.9, 155.9, 153.7 ($-\text{C}=\text{O}$), 153.1, 147.2, 145.6, 143.4, 138.9, 134.0, 130.0, 129.1, 128.6, 128.1, 127.2, 125.7, 122.0, 81.8 ($-\text{OC}(\text{CH}_3)_3$), 28.7 (CH_3).

$[\text{Ru}(\text{L}^8)_2](\text{PF}_6)_2$. obtained as red solid in 60% yield; Found: C, 57.97; H, 4.56; N, 7.83. Calc. for $\text{C}_{86}\text{H}_{82}\text{F}_{12}\text{N}_{10}\text{O}_8\text{P}_2\text{Ru}$: C, 58.20; H, 4.66; N, 7.89%; ^1H NMR (300 MHz, DMSO-d_6): δ 9.46 (s, 4 H; $\text{H}^{3',5'}$, terpy), 9.08 (d, $J = 8.2$ Hz, 4 H; $\text{H}^{3,3'}$, terpy), 8.39 (d, $J = 8.6$ Hz, 4 H), 8.07 (t, $J = 7.5$ Hz, 4 H; $\text{H}^{4,4'}$, terpy), 7.60–7.53 (m, 8 H), 7.43–7.38 (m, 4 H), 7.34–7.24 (m, 18 H; Ar), 1.48 (s, 18 H, $-\text{OC}(\text{CH}_3)_3$), 1.41 (s, 18 H, $-\text{OC}(\text{CH}_3)_3$); ^{13}C NMR (75 MHz, DMSO-d_6): δ 158.9, 155.9, 153.8 ($-\text{C}=\text{O}$), 153.6 ($-\text{C}=\text{O}$), 153.0, 147.2, 145.4, 143.5, 141.6, 140.8, 138.9, 134.1, 129.8, 129.2, 128.5, 128.3, 128.0, 126.9, 125.7, 122.0, 82.0 ($-\text{OC}(\text{CH}_3)_3$), 81.4 ($-\text{OC}(\text{CH}_3)_3$), 28.7 (CH_3).

$[\text{Ru}(\text{L}^9)_2](\text{PF}_6)_2$. obtained as deep red solid in 63% yield; Found: C, 59.74; H, 4.99; N, 7.74. Calc. for $\text{C}_{108}\text{H}_{108}\text{F}_{12}\text{N}_{12}\text{O}_{12}\text{P}_2\text{Ru}$: C, 60.13; H, 5.05; N, 7.79%; ^1H NMR (300 MHz, DMSO-d_6): δ 9.46 (s, 4 H; $\text{H}^{3',5'}$, terpy), 9.08 (d, $J = 8.1$ Hz, 4 H; $\text{H}^{3,3'}$, terpy), 8.39 (d, $J = 8.2$ Hz, 4 H), 8.08 (t, $J = 7.73$ Hz, 4 H; $\text{H}^{4,4'}$, terpy), 7.60–7.53 (m, 8 H), 7.40–7.23 (m, 30 H; Ar), 1.47 (s, 18 H, $-\text{OC}(\text{CH}_3)_3$), 1.41 (s, 18 H, $-\text{OC}(\text{CH}_3)_3$), 1.39 (s, 18 H, $-\text{OC}(\text{CH}_3)_3$); ^{13}C NMR (75 MHz, DMSO-d_6): δ 158.9, 155.9, 153.8 ($-\text{C}=\text{O}$), 153.6 ($-\text{C}=\text{O}$), 153.0, 147.2, 145.4, 143.5, 141.3, 140.9, 138.9, 134.1, 129.8, 129.2, 128.6, 128.4, 128.1, 128.0, 126.9, 125.6, 122.0, 82.0 ($-\text{OC}(\text{CH}_3)_3$), 81.6 ($-\text{OC}(\text{CH}_3)_3$), 81.4 ($-\text{OC}(\text{CH}_3)_3$), 28.6 (CH_3).

$[\text{Ru}(\text{L}^{10})_2](\text{PF}_6)_2$. obtained as deep red solid in 57% yield; Found: C, 61.19; H, 5.41; N, 7.51. Calc. for $\text{C}_{130}\text{H}_{134}\text{F}_{12}\text{N}_{14}\text{O}_{16}\text{P}_2\text{Ru}$: C, 61.48; H, 5.32; N, 7.72%; ^1H NMR (300 MHz, DMSO-d_6): δ 9.46 (s, 4 H; $\text{H}^{3',5'}$, terpy), 9.08 (d, $J = 8.3$ Hz, 4 H; $\text{H}^{3,3'}$, terpy), 8.38 (d, $J = 8.6$ Hz, 4 H), 8.06 (t, $J = 7.5$ Hz, 4 H; $\text{H}^{4,4'}$, terpy), 7.59–7.53 (m, 8 H), 7.33–7.19 (m, 38 H; Ar), 1.46 (s, 18 H, $-\text{OC}(\text{CH}_3)_3$), 1.40 (s, 18 H, $-\text{OC}(\text{CH}_3)_3$), 1.37 (s, 18 H, $-\text{OC}(\text{CH}_3)_3$), 1.35 (s, 18 H, $-\text{OC}(\text{CH}_3)_3$); ^{13}C NMR (75 MHz, DMSO-d_6): δ 158.9, 155.9, 153.8 ($-\text{C}=\text{O}$), 153.6 ($-\text{C}=\text{O}$), 153.1, 147.2, 145.4, 143.5, 141.3, 141.2, 141.1, 140.8, 138.9, 134.1, 129.7, 129.2, 128.5, 128.4, 128.1, 127.9, 126.8, 125.7, 122.0, 81.9 ($-\text{OC}(\text{CH}_3)_3$), 81.6 ($-\text{OC}(\text{CH}_3)_3$), 81.5 ($-\text{OC}(\text{CH}_3)_3$), 81.3 ($-\text{OC}(\text{CH}_3)_3$), 28.7, 28.6 (CH_3).

$[\text{Ru}(\text{L}^{13})_2](\text{PF}_6)_2$. obtained as red solid in 74% yield; Found: C, 56.97; H, 4.52; N, 8.36. Calc. for $\text{C}_{62}\text{H}_{56}\text{F}_{12}\text{N}_8\text{P}_2\text{Ru}$: C, 57.10; H, 4.33; N, 8.59%; ^1H NMR (300 MHz, DMSO-d_6): δ 9.25 (s, 4 H; $\text{H}^{3',5'}$, terpy), 8.95 (d, $J = 8.1$ Hz, 4 H; $\text{H}^{3,3'}$, terpy), 8.17 (d, $J = 8.9$ Hz, 4 H), 7.94 (t, $J = 8.4$ Hz, 4 H; $\text{H}^{4,4'}$, terpy), 7.42–7.35 (m, 8 H), 7.22–7.01 (m, 10 H), 6.99 (d, $J = 8.9$ Hz, 4 H; Ar), 3.78

(t, $J = 7.4$ Hz, 4 H, $\alpha(-\text{CH}_2)$), 1.58 (m, 4 H, $\beta(-\text{CH}_2)$), 1.32 (m, 4 H, $\gamma(-\text{CH}_2)$), 0.85 (t, $J = 7.3$ Hz, 6 H, $-\text{CH}_3$); ^{13}C NMR (75 MHz, DMSO-d_6): δ 159.1, 155.7, 152.9, 150.5, 147.8, 147.2, 138.7, 130.7, 129.6, 128.5, 126.0, 125.4, 120.6, 117.1, 52.2 ($\alpha(-\text{CH}_2)$), 30.1 ($\beta(-\text{CH}_2)$), 20.5 ($\gamma(-\text{CH}_2)$), 14.7 ($-\text{CH}_3$).

$[\text{Ru}(\text{L}^{14})_2](\text{PF}_6)_2$. obtained as deep red solid in 74% yield; Found: C, 61.72; H, 5.36; N, 8.51. Calc. for $\text{C}_{82}\text{H}_{82}\text{F}_{12}\text{N}_{10}\text{P}_2\text{Ru}$: C, 61.61; H, 5.17; N, 8.76%; ^1H NMR (300 MHz, DMSO-d_6): δ 9.34 (s, 4 H; $\text{H}^{3',5'}$, terpy), 9.04 (d, $J = 8.1$ Hz, 4 H; $\text{H}^{3,3'}$, terpy), 8.27 (d, $J = 8.5$ Hz, 4 H), 8.05 (t, $J = 7.7$ Hz, 4 H; $\text{H}^{4,4'}$, terpy), 7.51 (d, $J = 5.3$ Hz, 4 H), 7.35–7.20 (m, 12 H), 7.08–6.99 (m, 14 H; Ar), 3.83–3.72 (m, 8 H, $\alpha(-\text{CH}_2)$), 1.69–1.60 (m, 8 H, $\beta(-\text{CH}_2)$), 1.45–1.37 (m, 8 H, $\gamma(-\text{CH}_2)$), 0.99–0.90 (m, 12 H, $-\text{CH}_3$); ^{13}C NMR (75 MHz, DMSO-d_6): δ 158.3, 154.8, 152.1, 150.2, 147.5, 147.0, 145.0, 139.0, 137.8, 129.4, 128.7, 127.6, 127.3, 124.5, 124.1, 121.5, 121.2, 120.8, 119.4, 114.7, 67.0, 51.3 ($\alpha(-\text{CH}_2)$), 29.2 ($\beta(-\text{CH}_2)$), 19.6 ($\gamma(-\text{CH}_2)$), 13.9 ($-\text{CH}_3$).

General method for homo-dinuclear complexes

$[(\text{PTPY})\text{Ru}(\text{L})\text{Ru}(\text{PTPY})](\text{PF}_6)_4$ ($\text{L} = \text{L}^{11}$ and L^{12})

A suspension of ligand L^{11} or L^{12} and 2 eq. $[(\text{PTPY})\text{RuCl}_3]$ was heated at reflux in EtOH (200 cm^3) containing several drops of *N*-ethylmorpholine for 12 h. The reaction mixture was poured into aqueous NH_4PF_6 , and the precipitated solid was purified by column chromatography (silica gel, $\text{CH}_3\text{CN}/\text{sat.}$ aqueous $\text{KNO}_3/\text{H}_2\text{O}$). The major fraction was concentrated and ion-exchanged with aqueous NH_4PF_6 to precipitate the product as a red solid.

$[(\text{PTPY})\text{Ru}(\text{L}^{11})\text{Ru}(\text{PTPY})](\text{PF}_6)_4$. obtained as deep red solid in 58% yield; Found: C, 51.37; H, 3.49; N, 8.21. Calc. for $\text{C}_{100}\text{H}_{80}\text{F}_{24}\text{N}_{14}\text{O}_4\text{P}_4\text{Ru}_2$: C, 51.69; H, 3.47; N, 8.44%; ^1H NMR (300 MHz, DMSO-d_6): δ 9.51 (s, 4 H; $\text{H}^{3',5'}$, terpy), 9.49 (s, 4 H; $\text{H}^{3,5'}$, terpy), 9.12 (dd, $J = 8.52$ Hz, 8 H; $\text{H}^{3,3'}$, terpy), 8.45 (d, $J = 7.59$ Hz, 8 H), 8.09 (t, $J = 7.55$ Hz, 8 H; $\text{H}^{4,4'}$, terpy), 7.78 (d, $J = 7.11$ Hz, 4 H), 7.67 (m, 6 H), 7.57 (s, 8 H), 7.32 (s, 4 H), 7.30 (t, $J = 6.08$ Hz, 8 H; Ar), 1.51 (s, 18 H, $-\text{OC}(\text{CH}_3)_3$); ^{13}C NMR (75 MHz, DMSO-d_6): δ 158.9, 156.0, 153.7 ($-\text{C}=\text{O}$), 153.1, 148.0, 147.2, 145.4, 141.3, 138.9, 137.1, 134.3, 131.2, 130.3, 129.2, 128.6, 128.2, 125.7, 122.1, 82.0 ($-\text{OC}(\text{CH}_3)_3$), 28.8 ($-\text{CH}_3$).

$[(\text{PTPY})\text{Ru}(\text{L}^{12})\text{Ru}(\text{PTPY})](\text{PF}_6)_4$. obtained as deep red solid in 83% yield; Found: C, 53.87; H, 3.86; N, 8.59. Calc. for $\text{C}_{122}\text{H}_{106}\text{F}_{24}\text{N}_{16}\text{O}_8\text{P}_4\text{Ru}_2$: C, 54.15; H, 3.95; N, 8.28%; ^1H NMR (300 MHz, DMSO-d_6): δ 9.50 (s, 4 H; $\text{H}^{3',5'}$, terpy), 9.46 (s, 4 H; $\text{H}^{3,5'}$, terpy), 9.11 (dd, $J = 8.2$ Hz, 8 H; $\text{H}^{3,3'}$, terpy), 8.43 (dd, $J = 7.6$ Hz, 8 H), 8.07 (t, $J = 7.4$ Hz, 8 H; $\text{H}^{4,4'}$, terpy), 7.79 (t, $J = 7.1$ Hz, 4 H), 7.68 (t, $J = 8.1$ Hz, 2 H), 7.57 (m, 12 H), 7.31 (m, 20 H; Ar), 1.46 (s, 18 H, $-\text{OC}(\text{CH}_3)_3$), 1.41 (s, 18 H, $-\text{OC}(\text{CH}_3)_3$); ^{13}C NMR (75 MHz, DMSO-d_6): δ 158.9, 156.0, 153.8 ($-\text{C}=\text{O}$), 153.6 ($-\text{C}=\text{O}$), 153.1, 147.9, 147.2, 145.4, 141.3, 141.1, 140.9, 138.9, 137.0, 134.1, 131.2, 130.3, 129.2, 128.6, 128.2, 128.0, 125.7, 122.1, 82.0 ($-\text{OC}(\text{CH}_3)_3$), 81.6 ($-\text{OC}(\text{CH}_3)_3$), 28.7 ($-\text{CH}_3$).

General procedure for deprotection of ligands or complexes by thermolysis or by treatment with TMSI

The protected ligands or complexes were heated in a Schlenk tube under argon for 12 h at 185 $^\circ\text{C}$, and then cooled to

room temperature or treated with TMSI at room temperature in DCM or MeCN solution. The deprotected ligands or complexes were obtained as powders in quantitative yield, except $[(\text{PTPY})\text{Ru}(\text{L}^6)\text{Ru}(\text{PTPY})](\text{PF}_6)_4$.

L¹. Found: C, 81.05; H, 4.89; N, 14.02. Calc. for $\text{C}_{27}\text{H}_{20}\text{N}_4$: C, 80.98; H, 5.03; N, 13.99%; ¹H NMR (300 MHz, DMSO-*d*₆): δ 8.77 (d, *J* = 4.1 Hz, 2 H; H^{6,6'}, terpy), 8.69 (s, 2 H; H^{3',5'}, terpy), 8.67 (d, *J* = 7.4 Hz, 2 H; H^{3,3'}, terpy), 8.57 (s, 1 H, *N-H*), 8.03 (t, *J* = 8.5 Hz, 2 H; H^{4,4'}, terpy), 7.85 (d, *J* = 8.6 Hz, 2 H), 7.53 (dd, *J* = 5.0 Hz, 2 H; H^{5,5'}), 7.3 – 7.18 (m, 6 H), 6.93 (t, *J* = 7.2 Hz, 1 H; Ar); ¹³C NMR (75 MHz, DMSO-*d*₆): δ 156.4, 156.1, 150.1, 149.9, 146.1, 143.2, 138.2, 130.1, 128.7, 128.3, 125.2, 121.7, 119.0, 117.5, 117.0.

L². Found: C, 80.31; H, 4.99; N, 14.43. Calc. for $\text{C}_{33}\text{H}_{25}\text{N}_5$: C, 80.63; H, 5.13; N, 14.25%; ¹H NMR (300 MHz, DMSO-*d*₆): δ 8.76 (d, *J* = 4.2 Hz, 2 H; H^{6,6'}, terpy), 8.67 (s, 2 H; H^{3',5'}, terpy), 8.66 (d, *J* = 7.2 Hz, 2 H; H^{3,3'}, terpy), 8.33 (s, 1 H, *N-H*), 8.03 (t, *J* = 7.9 Hz, 2 H), 8.00 (s, 1 H, *N-H*), 7.80 (d, *J* = 8.7 Hz, 2 H), 7.52 (dd, *J* = 5.0 Hz, 2 H; H^{5,5'}, terpy), 7.20 (t, *J* = 7.5 Hz, 2 H), 7.13 – 7.00 (m, 8 H), 6.76 (t, *J* = 7.2 Hz, 1 H; Ar); ¹³C NMR (75 MHz, DMSO-*d*₆): δ 156.3, 156.2, 150.1, 147.6, 145.4, 138.5, 138.1, 135.9, 130.0, 128.6, 127.1, 125.1, 122.0, 121.7, 120.0, 119.6, 117.3, 116.4, 115.7.

L³. Found: C, 80.49; H, 4.87; N, 14.42. Calc. for $\text{C}_{39}\text{H}_{30}\text{N}_6$: C, 80.39; H, 5.19; N, 14.42%; ¹H NMR (300 MHz, DMSO-*d*₆): δ 8.76 (d, *J* = 4.7 Hz, 2 H; H^{6,6'}, terpy), 8.67 (s, 2 H; H^{3',5'}, terpy), 8.66 (d, *J* = 7.8 Hz, 2 H; H^{3,3'}, terpy), 8.24 (s, 1 H, *N-H*), 8.03 (t, *J* = 7.8 Hz, 2 H; H^{4,4'}, terpy), 7.81 (d, *J* = 5.7 Hz, 2 H), 7.79 (s, 1 H, *N-H*), 7.76 (s, 1 H, *N-H*), 7.52 (dd, *J* = 4.8 Hz, 2 H; H^{5,5'}, terpy), 7.16 (t, *J* = 7.4 Hz, 2 H), 7.09 (m, 4 H), 7.02 (m, 6 H), 6.93 (d, *J* = 7.7 Hz, 2 H), 6.70 (t, *J* = 7.2 Hz, 1 H; Ar).

L⁴. Found: C, 80.31; H, 5.11; N, 14.69. Calc. for $\text{C}_{45}\text{H}_{35}\text{N}_7$: C, 80.21; H, 5.24; N, 14.55%; ¹H NMR (300 MHz, DMSO-*d*₆): δ 8.76 (d, *J* = 4.7 Hz, 2 H; H^{6,6'}, terpy), 8.67 (s, 2 H; H^{3',5'}, terpy), 8.65 (d, *J* = 7.8 Hz, 2 H; H^{3,3'}, terpy), 8.22 (s, 1 H, *N-H*), 8.03 (t, *J* = 8.6 Hz, 2 H; H^{4,4'}, terpy), 7.78 (d, *J* = 8.8 Hz, 2 H), 7.76 (s, 1 H, *N-H*), 7.70 (s, 1 H, *N-H*), 7.63 (s, 1 H, *N-H*), 7.52 (dd, *J* = 6.3 Hz, 2 H; H^{5,5'}, terpy), 7.15 (t, *J* = 7.5 Hz, 2 H), 7.07 (m, 4 H), 6.98 (m, 12 H), 6.68 (t, *J* = 7.1 Hz, 1 H; Ar).

L⁵. Found: C, 79.34; H, 4.62; N, 15.34. Calc. for $\text{C}_{48}\text{H}_{34}\text{N}_8$: C, 79.76; H, 4.74; N, 15.50%; ¹H NMR (300 MHz, DMSO-*d*₆): δ 8.77 (d, *J* = 4.2 Hz, 4 H; H^{6,6'}, terpy), 8.69 – 8.65 (m, 8 H; H^{3',5',3,3'}, terpy), 8.41 (s, 2 H, *N-H*), 8.03 (t, *J* = 8.6 Hz, 4 H; H^{4,4'}, terpy), 7.82 (d, *J* = 8.6 Hz, 4 H), 7.52 (dd, *J* = 4.9 Hz, 4 H; H^{5,5'}, terpy), 7.20 – 7.17 (m, 8 H, Ar).

L⁶. Found: C, 79.29; H, 4.78; N, 15.55. Calc. for $\text{C}_{60}\text{H}_{44}\text{N}_{10}$: C, 79.62; H, 4.90; N, 15.48%; ¹H NMR (300 MHz, DMSO-*d*₆): δ 8.76 (d, *J* = 3.5 Hz, 4 H; H^{6,6'}, terpy), 8.66 – 8.64 (m, 8 H; H^{3',5',3,3'}, terpy), 8.19 (s, 2 H, *N-H*), 8.02 (t, *J* = 7.7 Hz, 4 H; H^{4,4'}, terpy), 7.78 (d, *J* = 8.6 Hz, 4 H), 7.70 (s, 2 H, *N-H*), 7.51 (dd, *J* = 4.7 Hz, 4 H; H^{5,5'}, terpy), 7.10 – 7.06 (m, 8 H), 7.01 – 6.98 (m, 8 H; Ar).

[Ru(L¹)₂](PF₆)₂. Found: C, 54.37; H, 3.30; N, 9.56. Calc. for $\text{C}_{54}\text{H}_{40}\text{F}_{12}\text{N}_8\text{P}_2\text{Ru}$: C, 54.41; H, 3.38; N, 9.40%; ¹H NMR (300 MHz, DMSO-*d*₆): δ 9.39 (s, 4 H; H^{3',5'}, terpy), 9.09 (d, *J* = 8.1 Hz, 4 H; H^{3,3'}, terpy), 8.79 (s, 2 H, *N-H*), 8.37 (d, *J* = 8.7 Hz,

4 H), 8.06 (t, *J* = 7.8 Hz, 4 H; H^{4,4'}, terpy), 7.54 (d, *J* = 5.4 Hz, 4 H), 7.39 (m, 8 H), 7.28 (m, 8 H), 7.01 (t, *J* = 7.5 Hz, 2 H; Ar).

[Ru(L²)₂](PF₆)₂. Found: C, 57.41; H, 3.62; N, 10.29. Calc. for $\text{C}_{66}\text{H}_{50}\text{F}_{12}\text{N}_{10}\text{P}_2\text{Ru}$: C, 57.69; H, 3.67; N, 10.19%; ¹H NMR (300 MHz, DMSO-*d*₆): δ 9.36 (s, 4 H; H^{3',5'}, terpy), 9.08 (d, *J* = 8.4 Hz, 4 H; H^{3,3'}, terpy), 8.56 (s, 2 H, *N-H*), 8.33 (d, *J* = 8.7 Hz, 4 H), 8.05 (m, 6 H), 7.53 (d, *J* = 5.4 Hz, 4 H), 7.27 – 7.06 (m, 20 H), 7.05 (d, *J* = 7.7 Hz, 4 H), 6.85 (t, *J* = 7.5 Hz, 2 H; Ar).

[Ru(L³)₂](PF₆)₂. Found: C, 60.30; H, 3.61; N, 11.20. Calc. for $\text{C}_{78}\text{H}_{60}\text{F}_{12}\text{N}_{12}\text{P}_2\text{Ru}$: C, 60.19; H, 3.89; N, 10.80%; ¹H NMR (300 MHz, DMSO-*d*₆): δ 9.35 (s, 4 H; H^{3',5'}, terpy), 9.07 (d, *J* = 8.2 Hz, 4 H; H^{3,3'}, terpy), 8.49 (s, 2 H, *N-H*), 8.31 (d, *J* = 8.5 Hz, 4 H), 8.05 (t, *J* = 7.7 Hz, 4 H; H^{4,4'}, terpy), 7.86 (s, 2 H, *N-H*), 7.85 (s, 2 H, *N-H*), 7.53 (d, *J* = 5.4 Hz, 4 H), 7.27 (t, *J* = 6.5 Hz, 4 H), 7.18 (m, 12 H), 7.11 (m, 12 H), 6.95 (d, *J* = 8.0 Hz, 4 H), 6.72 (t, *J* = 6.0 Hz, 2 H; Ar).

[Ru(L⁴)₂](PF₆)₂. Found: C, 61.91; H, 3.84; N, 11.31. Calc. for $\text{C}_{90}\text{H}_{70}\text{F}_{12}\text{N}_{14}\text{P}_2\text{Ru}$: C, 62.17; H, 4.06; N, 11.28%; ¹H NMR (300 MHz, DMSO-*d*₆): δ 9.40 (s, 4 H; H^{3',5'}, terpy), 9.08 (d, *J* = 7.6 Hz, 4 H; H^{3,3'}, terpy), 8.38 (d, *J* = 8.1 Hz, 4 H), 8.05 (t, *J* = 7.4 Hz, 4 H; H^{4,4'}, terpy), 7.54 (d, *J* = 3.6 Hz, 6 H), 7.42 – 6.89 (m, 40 H; Ar).

[(PTPY)Ru(L⁵)Ru(PTPY)](PF₆)₄. Found: C, 51.16; H, 2.97; N, 9.37. Calc. for $\text{C}_{90}\text{H}_{64}\text{F}_{24}\text{N}_{14}\text{P}_4\text{Ru}_2$: C, 50.90; H, 3.04; N, 9.23%; ¹H NMR (300 MHz, DMSO-*d*₆): δ 9.50 (s, 4 H; H^{3',5'}, terpy), 9.41 (s, 4 H; H^{3',5'}, terpy), 9.12 (dd, *J* = 7.4 Hz, 8 H; H^{3,3'}, terpy), 8.75 (s, 2 H, *N-H*), 8.42 (dd, *J* = 7.3 Hz, 8 H), 8.08 (t, *J* = 7.5 Hz, 8 H; H^{4,4'}, terpy), 7.81 – 7.56 (m, 15 H), 7.35 – 7.29 (m, 15 H; Ar).

Crystallography

[Ru(L¹³)₂](PF₆)₂. C₆₂H₅₆F₁₂N₈P₂Ru, MW = 1304.16, red needle, 0.28 × 0.16 × 0.05 mm³, triclinic, *P*1, *a* = 9.3421(14), *b* = 10.3691(15), *c* = 15.427(2) Å, α = 77.133(2), β = 89.628(2), γ = 80.524(2)°, *V* = 1436.3(4) Å³, *Z* = 1, *D*_{calcd} = 1.508 g/cm³, μ = 0.417 mm⁻¹. The intensity data were collected with the ω scan mode (186 K) on a Bruker Smart APEX diffractometer with CCD detector using Mo K α radiation (λ = 0.71073 Å). Lorentz, polarization factors were made for the intensity data and absorption corrections were performed using the SADABS program.⁴¹ The number of reflections collected was 8118, of which 6835 were independent (*R*_{int} = 0.0414). The crystal structures were solved using the SHELXTL program and refined using full matrix least squares.⁴² The positions of hydrogen atoms were calculated theoretically and included in the final cycles of refinement in a riding model along with attached carbons. The Flack parameter is 0.28(4) and 0.72(4) with the configuration inverted in space group *P*1, indicating that the complex is a twinned racemate crystal. *R*₁/*wR*₂ [*I* > 2 σ (*I*)]: 0.0593/0.1047. *R*₁/*wR*₂ [all reflections]: 0.0697/0.1100. *S* = 1.008. Residual electron density: 0.850 and –0.616 e Å⁻³.

Conclusion

In this study, a series of mono- and bis-topic terpyridine ligands and the corresponding mono- and bis-nuclear ruthenium(II) complexes have been successfully synthesized by incorporating

oligoaniline units at the *para*-position of a 4'-phenyl substituted terpyridine ligand. The palladium-catalyzed aromatic amination with Pd(OAc)₂/DPEphos as catalyst has proved to be an efficient method for synthesizing these compounds.

The introduction of electron-rich oligoaniline groups into electron-deficient terpyridine moieties can strengthen the donor-acceptor (D-A) interaction in Ru(II) complexes, resulting in much more intense and strongly red-shifted ¹MLCT bands in the absorption spectra. The ¹MLCT absorption maximum can be tuned over a span of 42 nm by changing the chain length and the substituent group in oligoaniline units. The shifts in potentials of the metal-based and oligoaniline-based oxidation waves suggest an interaction between the oligoaniline unit and the bis(terpyridine)-Ru²⁺ center. The dinuclear complexes with oligoaniline units as spacers possess higher ¹MLCT energy levels than the corresponding mononuclear complexes, while no apparent electronic coupling between two Ru²⁺ centers is observed.

Moreover, with incorporation of photo- and electro-active oligoaniline units, the ligands and Ru(II) complexes are endowed with other interesting properties. The characteristic absorption bands in the visual and NIR scales, relating to various states of oligoaniline units (*n* = 3, 4) in ligands and complexes, are easily modulated by the oxidation and doping effect. Single aniline moiety in Ru(II) complexes trigger the oxidative electropolymerization reaction to form a hybrid polymer film on the electrode surface. The Ru(II) complexes with longer oligoaniline chains are provided with multiplicate redox processes based on various components. All of these unique spectroscopic and redox properties suggest that this novel class of Ru(II) complexes is worthy of further investigation for photoelectronic materials.

Acknowledgements

This work is supported by the National Natural Science Foundation of China (No. 20874098 and 50673088), Science Fund for Creative Research Groups (No. 20621401) and 973 Project (2002CB613400).

References

- U. S. Schubert, H. Hofmeier, G. R. Newkome, in *Modern Terpyridine Chemistry*, Wiley-VCH, Weinheim, 2006.
- (a) U. S. Schubert and C. Eschbaumer, *Angew. Chem. Int. Ed.*, 2002, **41**, 2892; (b) E. C. Constable, R. W. Handel, C. E. Housecroft, A. F. Morales, B. Ventura, L. Flamigni and F. Barigelletti, *Chem. Eur. J.*, 2005, **11**, 4024; (c) W. Lu, Y.-C. Law, J. Han, S. S.-Y. Chui, D.-L. Ma, N. Zhu and C.-M. Che, *Chem. Asian J.*, 2008, **3**, 59.
- (a) M. Heller and U. S. Schubert, *Eur. J. Org. Chem.*, 2003, 947; (b) M. I. J. Polson, E. A. Medlycott, G. S. Hanan, L. Mikelsons, N. J. Taylor, M. Watanabe, Y. Tanaka, F. Loiseau, R. Passalacqua and S. Campagna, *Chem. Eur. J.*, 2004, **10**, 3640; (c) M. A. Halcrow, *Coord. Chem. Rev.*, 2005, **249**, 2880; (d) J. Wang, Y.-Q. Fang, L. B. Merle, M. I. J. Polson, G. S. Hanan, A. Juris, F. Loiseau and S. Campagna, *Chem. Eur. J.*, 2006, **12**, 8539; (e) Y.-Q. Fang, N. J. Taylor, F. Laverdière, G. S. Hanan, F. Loiseau, F. Nastasi, S. Campagna, H. Nierengarten, E. L. Wagner and A. V. Dorsselaer, *Inorg. Chem.*, 2007, **46**, 2854.
- (a) A. M. W. C. Thompson, *Coord. Chem. Rev.*, 1997, **160**, 1; (b) E. Breuning, G. S. Hanan, F. J. R. Salguero, A. M. Garcia, P. N. W. Baxter, J.-M. Lehn, E. Wegelius, K. Rissanen, H. Nierengarten and A. van Dorsselaer, *Chem. Eur. J.*, 2002, **8**, 3458; (c) P. R. Andres and U. S. Schubert, *Adv. Mater.*, 2004, **16**, 1043; (d) E. A. Medlycott and G. S. Hanan, *Coord. Chem. Rev.*, 2006, **250**, 1763; (e) M. W. Cooke, G. S. Hanan, F. Loiseau, S. Campagna, M. Watanabe and Y. Tanaka, *J. Am. Chem. Soc.*, 2007, **129**, 10479.
- L. Hammarström, F. Barigelletti, L. Flamigni, N. Armaroli, A. Sour, J.-P. Collin and J.-P. Sauvage, *J. Am. Chem. Soc.*, 1996, **118**, 11972.
- (a) T. Yutaka, M. Kurihara, K. Kubo and H. Nishihara, *Inorg. Chem.*, 2000, **39**, 3438; (b) T. Yutaka, I. Mori, M. Kurihara, J. Mizutani, K. Kubo, S. Furusho, K. Matsumura, N. Tamai and H. Nishihara, *Inorg. Chem.*, 2001, **40**, 4986; (c) T. Yutaka, I. Mori, M. Kurihara, N. Tamai and H. Nishihara, *Inorg. Chem.*, 2003, **42**, 6306.
- (a) F. Barigelletti, L. Flamigni, V. Balzani, J.-P. Collin, J.-P. Sauvage, A. Sour, E. C. Constable and A. M. W. C. Thompson, *J. Am. Chem. Soc.*, 1994, **116**, 7692; (b) M. T. Indelli, F. Scandola, J.-P. Collin, J.-P. Sauvage and A. Sour, *Inorg. Chem.*, 1996, **35**, 303; (c) M. T. Indelli, F. Scandola, L. Flamigni, J.-P. Collin, J.-P. Sauvage and A. Sour, *Inorg. Chem.*, 1997, **36**, 4247; (d) F. Barigelletti, L. Flamigni, J.-P. Collin and J.-P. Sauvage, *Chem. Commun.*, 1997, 333; (e) A. Auffrant, A. Barbieri, F. Barigelletti, J.-P. Collin, L. Flamigni, C. Sabatini and J.-P. Sauvage, *Inorg. Chem.*, 2006, **45**, 10990.
- V. Grosshenny, A. Harriman, J.-P. Gisselbrecht and R. Ziessel, *J. Am. Chem. Soc.*, 1996, **118**, 10315.
- (a) M. Hissler, A. El-ghayoury, A. Harriman and R. Ziessel, *Angew. Chem. Int. Ed.*, 1998, **37**, 1717; (b) A. El-ghayoury, A. Harriman, A. Khatyr and R. Ziessel, *Angew. Chem. Int. Ed.*, 2000, **39**, 185; (c) A. Harriman, A. Khatyr, R. Ziessel and A. C. Benniston, *Angew. Chem. Int. Ed.*, 2000, **39**, 4287.
- (a) E. C. Constable, C. E. Housecroft, E. R. Schofield, S. Encinas, N. Armaroli, F. Barigelletti, L. Flamigni, E. Figgemerier and J. G. Vos, *Chem. Commun.*, 1999, 869; (b) S. Encinas, L. Flamigni, F. Barigelletti, E. C. Constable, C. E. Housecroft, E. R. Schofield, E. Figgemerier, D. Fenske, M. Neuburger, J. G. Vos and M. Zehnder, *Chem.-Eur. J.*, 2002, **8**, 137.
- A. Barbieri, B. Ventura, F. Barigelletti, A. De Nicola, M. Quesada and R. Ziessel, *Inorg. Chem.*, 2004, **43**, 7359.
- (a) T.-Y. Dong, M. Lin and Y. N. Chiang, *Inorg. Chem. Commun.*, 2004, **7**, 687; (b) T.-Y. Dong, H.-W. Shih and L.-S. Chang, *Langmuir*, 2004, **20**, 9340; (c) T.-Y. Dong, K. Chen, M.-C. Lin and L. Lee, *Organometallics*, 2005, **24**, 4198.
- F. Barigelletti, L. Flamigni, M. Guardigli, A. Juris, M. Beley, S. C. Kimmes, J.-P. Collin and J.-P. Sauvage, *Inorg. Chem.*, 1996, **35**, 136.
- (a) Y. Yang and A. J. Heeger, *Nature (London)*, 1994, **372**, 344; (b) A. R. Brown, A. Pomp, C. M. Hart and D. M. Leeuw, *Science*, 1995, **270**, 972; (c) M. Granstrom, M. Berggren and O. Inganäs, *Science*, 1995, **267**, 1479; (d) M. Berggren, A. Dodabalapur, R. E. Slusher and Z. Bao, *Nature (London)*, 1997, **389**, 466; (e) G. Horowitz, *Adv. Mater.*, 1998, **10**, 365; (f) B. Crone, A. Dodabalapur, A. Gelperin, L. Torsi, H. E. Katz, A. J. Lovinger and Z. Bao, *Appl. Phys. Lett.*, 2001, **78**, 2229.
- J. P. Sadighi, R. A. Singer and S. L. Buchwald, *J. Am. Chem. Soc.*, 1998, **120**, 4960.
- (a) F.-L. Lu, F. Wudl, M. Nowak and A. J. Heeger, *J. Am. Chem. Soc.*, 1986, **108**, 8311; (b) F. Wudl, R. O. Angus, F. L. Lu, P. M. Allemand, D. J. Vachon, M. Nowak, Z. X. Liu and A. J. Heeger, *J. Am. Chem. Soc.*, 1987, **109**, 3677; (c) M. Ochi, H. Furusho and J. Tanaka, *Bull. Chem. Soc. Jpn.*, 1994, **67**, 1749; (d) E. Rebourt, J. A. Joule and A. P. Monkman, *Synth. Met.*, 1997, **84**, 65; (e) W. J. Zhang, J. Feng, A. G. MacDiarmid and A. J. Epstein, *Synth. Met.*, 1997, **84**, 119.
- (a) J. P. Wolfe, S. Wagaw and S. L. Buchwald, *J. Am. Chem. Soc.*, 1996, **118**, 7215; (b) M. S. Driver and J. F. Hartwig, *J. Am. Chem. Soc.*, 1996, **118**, 7217; (c) R. A. Singer, J. P. Sadighi and S. L. Buchwald, *J. Am. Chem. Soc.*, 1998, **120**, 213.
- (a) A. S. Guram and S. L. Buchwald, *J. Am. Chem. Soc.*, 1994, **116**, 7901; (b) A. S. Guram, R. A. Rennels and S. L. Buchwald, *Angew. Chem. Int. Ed. Engl.*, 1995, **34**, 1348; (c) J. P. Wolfe and S. L. Buchwald, *J. Org. Chem.*, 1996, **61**, 1133; (d) J. P. Sadighi, M. C. Harris and S. L. Buchwald, *Tetrahedron. Lett.*, 1998, **39**, 5327.
- R. Chen and B. C. Benicewicz, *Macromolecules*, 2003, **36**, 6333.
- F. Krönke, *Synthesis*, 1976, **1**, 1.
- V. H. Rawal, R. J. Jones and M. P. Cava, *J. Org. Chem.*, 1987, **52**, 19.
- R. S. Lott, V. S. Chauhan and C. H. Stammer, *J. Chem. Soc., Chem. Commun.*, 1979, 495.
- (a) G. D. Storrer, S. B. Colbran and D. C. Craig, *J. Chem. Soc. Dalton Trans.*, 1997, 3011; (b) A. Barbieri, B. Ventura, F. Barigelletti, A. De Nicola, M. Quesada and R. Ziessel, *Inorg. Chem.*, 2004, **43**, 7359.
- C. G. Bochet, C. Pigué and A. F. Williams, *Helv. Chim. Acta.*, 1993, **76**, 372.
- M. Maestri, N. Armaroli, V. Balzani, E. C. Constable and A. M. W. C. Thompson, *Inorg. Chem.*, 1995, **34**, 2759.

- 26 (a) W. Zheng, M. Angelopoulos, A. J. Epstein and A. J. MacDiarmid, *Macromolecules*, 1997, **30**, 7634; (b) X.-X. Zhang, J. P. Sadighi, T. W. Mackewitz and S. L. Buchwald, *J. Am. Chem. Soc.*, 2000, **122**, 7606; (c) R. E. Ward and T. Y. Meyer, *Macromolecules*, 2003, **36**, 4368; (d) J. Gong, J. H. Yang, X. J. Cui, S. G. Wang, Z. M. Su and L. Y. Qu, *Synth. Met.*, 2002, **129**, 15; (e) C.-W. Lee, Y.-H. Seo and S.-H. Lee, *Macromolecules*, 2004, **37**, 4070; (f) C. Querner, P. Reiss, J. Bleuse and A. Pron, *J. Am. Soc. Chem.*, 2004, **126**, 11574.
- 27 J. Y. Shimano and A. G. MacDiarmid, *Synth. Met.*, 2001, **123**, 251.
- 28 W. S. Huang and A. G. MacDiarmid, *Polymer*, 1993, **34**, 1833.
- 29 (a) L. W. Shacklette, J. F. Wolf, S. Gould and R. H. Banghman, *J. Chem. Phys.*, 1988, **88**, 3955; (b) T. Moll and J. Heinze, *Synth. Met.*, 1993, **55–57**, 1521.
- 30 M.-Y. Chou, M.-K. Leung, Y. O. Su, C. L. Chiang, C.-C. Lin, J.-H. Liu, C.-K. Kuo and C. Y. Mou, *Chem. Mater.*, 2004, **16**, 654.
- 31 F. Chen, C. Nuckolls and S. Lindsay, *Chem. Phys.*, 2006, **324**, 236.
- 32 J. F. Wolf, C. E. Forbes, S. Gould and L. W. Shacklette, *J. Electrochem. Soc.*, 1989, **136**, 2887.
- 33 M. M. Wienk and R. A. J. Janssen, *J. Am. Chem. Soc.*, 1996, **118**, 10626.
- 34 A. E. Pullen and T. M. Swager, *Macromolecules*, 2001, **34**, 812.
- 35 F. E. Goodson, S. I. Hauck and J. F. Hartwig, *J. Am. Chem. Soc.*, 1999, **121**, 7527.
- 36 E. C. Constable and A. M. W. C. Thompson, *J. Chem. Soc. Dalton Trans.*, 1995, 1615.
- 37 G. D. Storrier and S. B. Colbran, *J. Chem. Soc. Dalton Trans.*, 1996, 2185.
- 38 J. Hjelm, R. W. Handel, A. Hagfeldt, E. C. Constable, C. E. Housecroft and R. J. Forster, *Inorg. Chem.*, 2005, **44**, 1073.
- 39 (a) J. Pommerehne, H. Vestweber, W. Guss, R. F. Mahrt, H. Bässler, M. Porsch and J. Daub, *Adv. Mater.*, 1995, **7**, 551; (b) S. Ranjan, S.-Y. Lin, K.-C. Hwang, Y. Chi, W.-L. Ching, C.-S. Liu, Y.-T. Tao, C.-H. Chien, S.-M. Peng and G.-H. Lee, *Inorg. Chem.*, 2003, **42**, 1248.
- 40 (a) R. M. Leasure, W. Ou, J. A. Moss, R. W. Linton and T. J. Meyer, *Chem. Mater.*, 1996, **8**, 264; (b) R. P. Kingsborough and T. M. Swager, *J. Am. Chem. Soc.*, 1999, **121**, 8825; (c) P. G. Pickup, *J. Mater. Chem.*, 1999, **9**, 1641; (d) M. O. Wolf, *Adv. Mater.*, 2001, **13**, 545.
- 41 R. H. Blessing, *Acta Crystallogr.*, 1995, **A51**, 33.
- 42 G. M. Sheldrick, *SHELXTL*, version 5.1; Bruker Analytical X-ray Systems, Inc.: Madison, WI, 1997.